



# Groundwater chemistry and health hazard risk valuation of fluoride and nitrate enhanced groundwater from a semi-urban region of South India

Ratnakar Dhakate<sup>1,2</sup> · Shekhar More<sup>1,2</sup> · Laxman Kumar Duvva<sup>3</sup> · Satyanarayana Enjamuri<sup>4</sup>

Received: 27 August 2022 / Accepted: 9 January 2023 / Published online: 20 January 2023  
© The Author(s), under exclusive licence to Springer-Verlag GmbH Germany, part of Springer Nature 2023

## Abstract

Evaluation of groundwater chemistry and its related health hazard risk for humans is a prerequisite remedial measure. The semi-urban region in southern India was selected to measure the groundwater quality to know the human health risk valuation for different age groups of adults and children through oral intake and skin contact with elevated concentrations of fluoride ( $F^-$ ) and nitrate ( $NO_3^-$ ) groundwater. Groundwater samples were collected from the semi-urban region for pre- and post-rainfall periods and resolute its major ion chemistry. The pH values showed the water is alkaline to neutral in nature. Total dissolved solid (TDS) ranged from 201 to 3612 mg/l and 154 to 3457 mg/l. However,  $F^-$  concentration ranges from 0.28 to 5.48 mg/l and 0.21 to 4.43 mg/l; and  $NO_3^-$  ranges from 0.09 to 897.28 mg/l and 0.0 to 606.10 mg/l elevating the drinking water standards of  $F^-$  in 32% and 38% samples and for  $NO_3^-$  about 62% and 38% during pre- and post-rainfall seasons, respectively. The fluoride-bearing minerals are the main sources of elevated concentrations of  $F^-$  and excessive use of chemical fertilizers as the chief source of  $NO_3^-$  concentration in the aquifer regime. Water quality index (WQI) ranged from 18.3 to 233 and 12.97 to 219.14; 20% and 22% showed poor water quality for pre- and post-rainfall seasons with  $WQI \geq 200$ . Piper plot suggests that 46% and 51% of samples signify carbonate water type ( $Ca^{2+} - HCO_3^-$ ), and 32% and 28% of groundwater samples show ( $Ca^{2+} + Na^+ + HCO_3^-$ ) type water for pre- and post-rainfall seasons respectively. Gibbs' plot suggests the dominance of water–rock interaction in the aquifer system. Further, the principal component analysis (PCA) revealed three and four components which explain 74.85% and 79.30% of the variance in pre- and post-rainfall seasons with positive loading of EC, TDS,  $Ca^{2+}$ ,  $Na^+$ ,  $Mg^{2+}$ ,  $K^+$ ,  $SO_4^{2-}$ ,  $Cl^-$ , and  $HCO_3^-$  due to mineral weathering and water–rock interactions altering the chemistry for an elevated concentration of  $F^-$  and  $NO_3^-$  in groundwater. Cluster analyses of chemical variables observed four clusters with a linkage distance of 5 to 25 with a linkage between different variables displaying predominant ion exchange, weathering of silicate and fluoride-rich minerals, salinization of the water, and a high value of  $NO_3^-$  concentration, resulting from fertilizers. The hazard quotient (HQ) through ingestion ( $HQ_{ing}$ ) and dermal ( $HQ_{der}$ ) pathways of  $F^-$  and  $NO_3^-$  was observed higher than its acceptable limit of 1.0 for different age groups indicating the non-carcinogenic effect on human health. Effective strategic measures like defluoridation, denitrification, safe drinking water supply, sanitary facilities, and rainwater harvesting structures are to be implemented in the area for improvement of human health conditions and also bring awareness to the local community about the health hazard effects of using high concentrated  $F^-$  and  $NO_3^-$  water for daily uses.

**Keywords** Water quality index (WQI) · Hazard quotient (HQ) · Human health hazard · Health risk assessment · Principal component analyses (PCA)

Responsible Editor: Xianliang Yi

✉ Ratnakar Dhakate  
dhakate.ratnakar@gmail.com

Extended author information available on the last page of the article

## Introduction

Groundwater is the prime reserve exploited for drinking and irrigation uses in arid and semi-arid regions of the globe. Most of the domestic water is met from groundwater reserves in urban and rural areas of India (Ali et al. 2019). Due to anthropogenic exercises like rapid growth in population, urban development, expansion of industrial areas,

additional fertilizers application in the irrigated field, meager sewage system, dumping of human and animal waste, and due to geogenic processes, groundwater is getting polluted.

F<sup>-</sup> and NO<sub>3</sub><sup>-</sup> contamination in groundwater is a major concern globally and several studies have been conducted to relate irrigation practices and enrichment of NO<sub>3</sub><sup>-</sup> pollution in groundwater regimes (Adimalla et al. 2019; Kumar et al. 2019; Mas-Pla and Menció 2019; Pérez Villarreal et al. 2019; Gao et al. 2020; Zhang et al. 2020). Similarly, a high fluoride content in groundwater was reported in India (Sudheer Kumar et al. 2017; Satyanarayana et al. 2017; Laxman-kumar et al. 2019; Adimalla and Li 2019; Bera and Ghosh 2019; Katla et al. 2021). The first fluoride contamination in water was reported in India in the year 1937 in the Nellore district of Andhra Pradesh. Peoples all over the world suffer from a disease called fluorosis due to the ingestion of elevated concentrations of F<sup>-</sup> water in the absence of an alternative source (Farooq et al. 2018; Adimalla et al. 2019). About nine districts of Telangana state are suffering from high F<sup>-</sup> content in water (CGWB 2018). Telangana state is mostly covered by granitic rock, which mainly consists of F<sup>-</sup>-bearing minerals and is the major cause of F<sup>-</sup> occurrence in groundwater (Machender et al. 2014; Satyanarayana et al. 2017; Laxman Kumar et al. 2019; Adimalla et al. 2019).

In recent years, NO<sub>3</sub><sup>-</sup> contamination in groundwater became a prominent issue throughout the globe and many investigations carried out by various researchers in India and worldwide to recognize a significant relationship between irrigation practices and waste disposal practices for the enhancement of NO<sub>3</sub><sup>-</sup> concentration levels in groundwater regime (Pérez Villarreal et al. 2019; Adimalla 2020; Gao et al. 2020; Zhang et al. 2020). The studies carried out by Pérez Villarreal et al. (2019) found that the high NO<sub>3</sub><sup>-</sup> concentration was due to agricultural practices and municipal wastewater flowing in the urban region of Mexico. Zhang et al. (2020) observed the spread and cause of NO<sub>3</sub><sup>-</sup> in groundwater of urban regions of China and found that the majority of the aquifers contaminated with NO<sub>3</sub><sup>-</sup> concentration were due to leakage of domestic sewage and construction regions. Similarly, groundwater in the middle Gangetic plain of India also reported an elevated concentration of NO<sub>3</sub><sup>-</sup>, and it is controlled by excessive use of fertilizers, livestock activity, and seepage from septic tanks (Kumar et al. 2019).

Continuous intake of F<sup>-</sup> and NO<sub>3</sub><sup>-</sup> polluted drinking water causes serious health risks to children and adults. Consequently, health risk assessment studies linked with F<sup>-</sup> and NO<sub>3</sub><sup>-</sup> are widely studied in different parts of India (Adimalla and Qian 2019; Adimalla et al. 2019, 2020; Adimalla 2020; Karunanidhi et al. 2020), and in different parts of the world like Iran (Qasemi et al. 2018; Yousefi et al. 2018), Pakistan (Rehman et al. 2020), China (Chen et al. 2017a, b; Su et al. 2018; Gao et al. 2020), and Mexico (Pérez Villarreal et al. 2019) have attention on the non-carcinogenic risk for children

and adults. All these studies found that children are at more risk than adults.

Nowadays, there is a growing concern about groundwater quality and its effects on human well-being (More et al. 2021). The studies related to groundwater chemistry for irrigation purposes, assessment of stream water quality and health risk assessment, sediment contamination of stream water, and water quality evaluation by the biological approach have been demonstrated by using geochemical evaluation and multivariate statistical methods (Ustaoglu and Tepe 2019; Ustaoglu et al. 2020; Aydin et al. 2021; Tasa et al. 2019; Gugulothu et al. 2022a). The United States Environmental Protection Agency (USEPA) has established a model, policies, and guiding principle for the human health risk assessment (HRA) (U.S. EPA 2011) to assess and understand the significance of human health through diverse pathways. It is broadly accepted by different researchers all over the world to define the adverse effects on human health due to intake of high F<sup>-</sup> and NO<sub>3</sub><sup>-</sup> contaminated water (Narsimha and Rajitha 2018; Karunanidhi et al. 2020; Zango et al. 2019; Yuan et al. 2020).

The present study area is a part of the semi-urban region of Mulugu and Venkatapur mandals of Warangal District, Telangana State, India. Residents of this area mainly depend upon the groundwater for their daily uses due to the lack of a supply water scheme. Intensive and long-term practices of unlimited usage of chemical fertilizers and animal waste influence groundwater quality. Further, the sanitary facilities and disposal of household waste have poor conditions in the area. These factors are well-known contaminated sources for elevating the groundwater concentrations levels of F<sup>-</sup> and NO<sub>3</sub><sup>-</sup> contents, since there is no research study carried out so far, for the assessment of the sources and origin of inferior groundwater quality in the Mulugu and Venkatapur mandals of Warangal district, Telangana State, India. Therefore, the main aims of the present study are the assessment of (a) the sources and origin of the inferior groundwater quality; (b) to assess the groundwater for drinking suitability using Piper's trilinear diagram, rock–water interaction, and identify the sources and factor controlling the groundwater chemistry by principal component analysis; and (c) health risk problems related to consumption of high F<sup>-</sup> and NO<sub>3</sub><sup>-</sup> groundwater through ingestion and dermal pathways for different age groups of people viz., 6 to 12 months, 6 to 11 years, 11 to 16 years, 16 to 18 years, 18 to 21 years, ≥ 21 years, and ≥ 65 years by applying the recommended method suggested by the USEPA.

## Study area and its geology

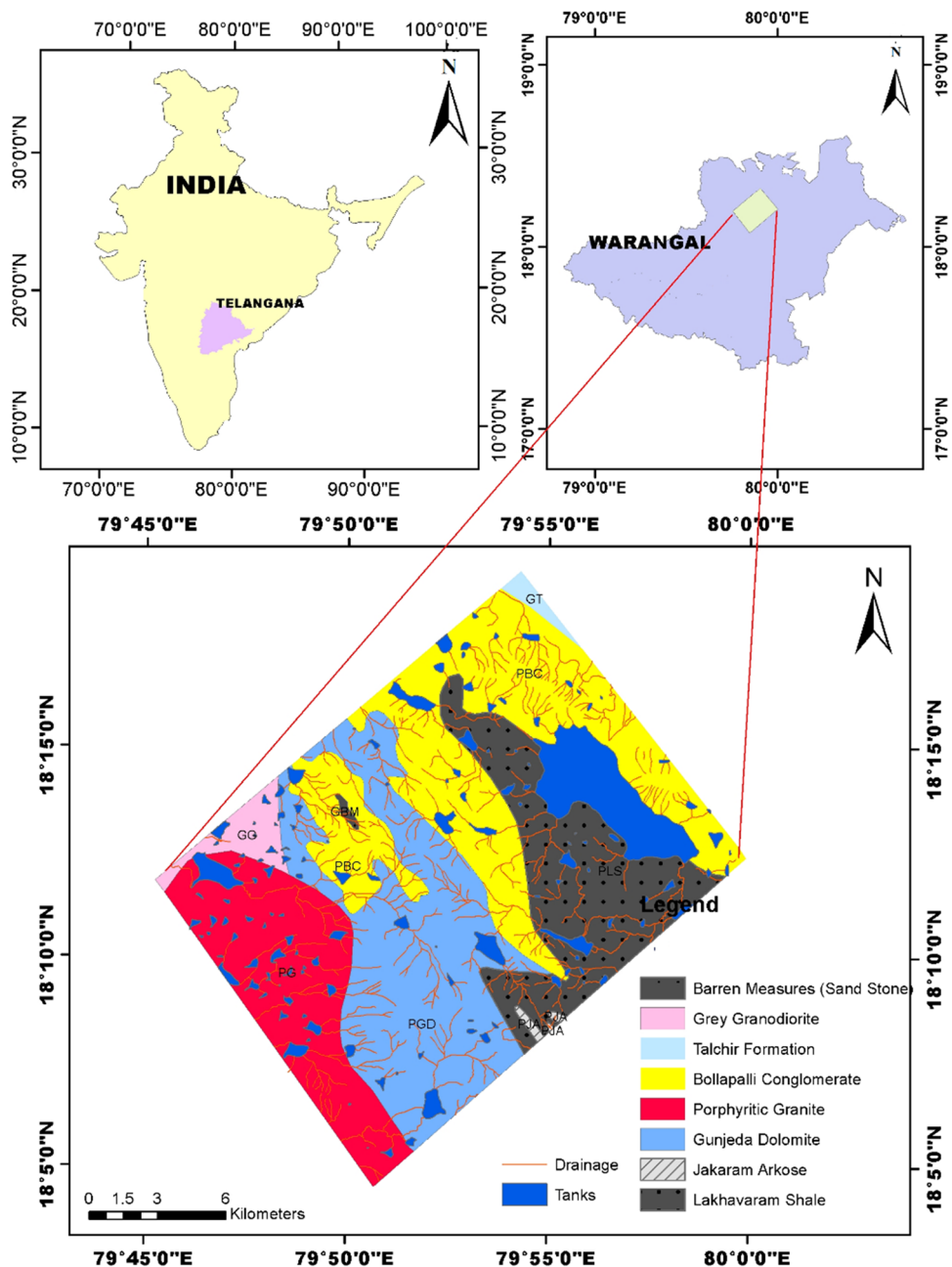
The study area belongs to Mulugu and Venkatapur mandals of Warangal district, Telangana State. It is located 50 km away to the northeast of Warangal City and covers a

semi-arid zone and comes under Survey of India Toposheet No. 56 N/15 and 56 N/16 with an extent of 453 sq. km (Fig. 1). The area has a moderate slope from NW to SE direction and NE to SE direction. The temperature gradually rises from 30 to 38 °C during the month of February to May and decreases from 8 to 10 °C during the month of June to December. Rains generally occurred during June to October months and the average annual rainfall is 994 mm. About 80% of the rainfall is contributed from the southwest monsoon. The drainage pattern is dendritic and rectangular in nature controlled by uneven terrain. Groundwater occurs in the soil of weathered granite, semi-weathered, fractured hard

rock, and in weathered sedimentary formations under the water table in semi-confined conditions. The average depth of groundwater is about 8–10 m. The granite rocks possess negligible primary porosity, but in sedimentary rock the secondary porosity exits by deep fracturing and weathering, they are rendered with porosity and permeability, which locally form potential aquifers in the study area (CGWB 2018).

Geologically, the study area covers a part of the stable Southern Indian shield consisting of the Peninsular Gneissic Complex (PGC) consisting of gneisses, granite and dolerite dykes, Pakhal group, and Mulugu subgroup. The Mulugu subgroup occupies a major part of the study area and comprises

**Fig. 1** Location map showing the geology of the study area



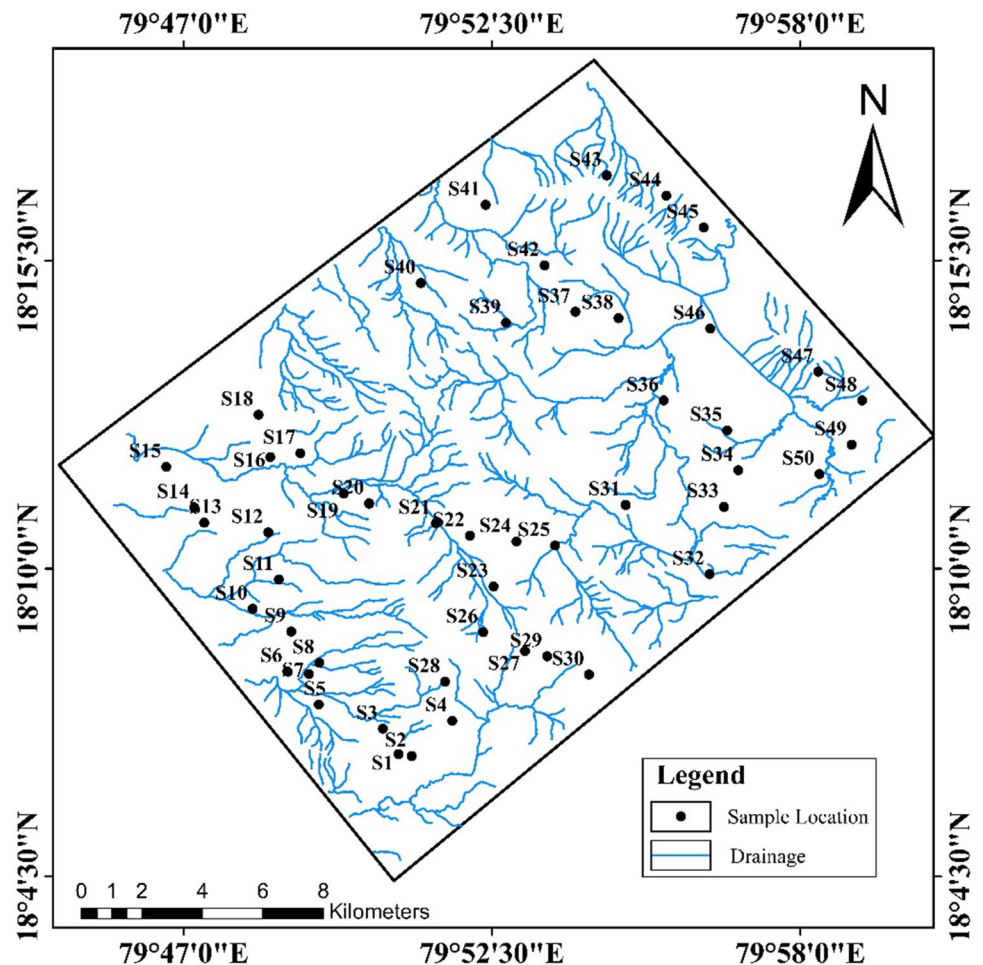
Arkose, shale with dolomite quartzite, shale, quartzite, limestone, and sandstone. In the study area, the Archaean peninsular gneissic complex is unconformably overlain by sedimentary rocks of the Middle Proterozoic age, consisting of the Pakhal group of rocks. The reddish-brown soil cover is a result of well-developed residual of weathered granite. The soil is fairly permeable, and the infiltration rate can absorb most of the rain except for more intensive rains, which can cause considerable surface flow and erosion (GSI 1995). The geological map of the study area is shown in Fig. 1.

### Materials and methods

Shallow dug wells, hand pumps, and deep bore wells were selected to collect the water samples following the standards procedures (APHA 2012) during pre- and post-rainfall season and their locations are shown in Fig. 2. Samples were stored in the laboratory at 4 °C and filtered with 0.45 μ Whatman Filter paper before the analyses. Water samples were analyzed at the laboratory of Centre for Materials for Electronics Technology (C-MET), Hyderabad for physico-chemical (pH, EC, TDS, and

TH), and major ions (cations  $Ca^{2+}$ ,  $Mg^{2+}$ ,  $Na^+$ ,  $K^+$ , and anions  $Cl^-$ ,  $SO_4^{2-}$ ,  $F^-$ ,  $NO_3^-$ , and  $HCO_3^-$ ) chemistry. The pH was measured using the digital pH meter of Elico; EC was estimated by the EC analyzer CM 183 model of ELICO; classical methods of analysis were applied for the estimation of  $Ca^{2+}$ ,  $Mg^{2+}$ , and  $Cl^-$ .  $Na^+$  and  $K^+$  were analyzed by flame photometry using CL-345 flame photometer of ELICO.  $SO_4^{2-}$  was estimated by the turbidity method using the Digital Nephelo-Turbidity meter 132 model of Systronics.  $NO_3^-$  was analyzed applying the UV–Vis screen method using the UV–Vis spectrophotometer UV-1201 model of Shimadzu.  $F^-$  was analyzed by the ion selective electrode method using Orion 290A + model of Thermo-electron Corporation. The TDS were estimated by the summation of cations and anions (epm) method (Hem 1985). The charge balance is calculated between cations and anions and is within acceptable limits confirming the reliability of analytical results with precision of  $\pm 5\%$  for all the samples. The quality of the analysis was ensured by standardization using blank, spike, and duplicate samples. Standard titration method was used for bicarbonates (BIS 2012). The statistical summary of major ion of groundwater samples for pre- and post-rainfall seasons is given in Table 1.

Fig. 2 Groundwater sample locations in the study area



### Groundwater suitability for drinking

Water quality index (WQI) is a comprehensive method to prompt the complete quality of drinking water in a single measurement (Subba Rao et al. 2020; Wu et al. 2020). The first stage is to determine the relative weight ( $W_i$ ) of each chemical characteristic based on its relative impact on human health after allocating the unit weight ( $w_i$ ) (Eq. 1). The next stage is the calculation of the water quality rating ( $q_i$ ), which is done by dividing the concentration of each chemical parameter ( $C_i$ ) by the standard for drinking water quality ( $S_i$ ) (Eq. 2). In the third stage, assessment of  $SI_i$  by multiplying  $q_i$  with  $W_i$  to the individual chemical parameter (Eq. 3), and in the final stage, we get  $WQI$  by computation of summation of all  $SI_i$  of individual samples (Eq. 4).

$$W_i = \frac{w_i}{\sum_{n=1}^n w_i} \tag{1}$$

$$q_i = \frac{C_i}{S_i} \times 100 \tag{2}$$

$$SI_i = q_i \times W_i \tag{3}$$

$$WQI = \sum_{i=1}^n SI_i \tag{4}$$

If the WQI value is < 50, it indicates the excellent quality of water; if it ranges between > 50 and < 100, it indicates good quality water; if it ranges between > 100 and < 200, it indicates poor quality water; if it ranges between > 200 and < 300,

it indicates very poor-quality water; and if it is > 300, it recommends unfit water quality for ingestion purpose.

### Water facies

The Piper diagram comprises of cation and anion in two triangle parts and a central diamond-shaped part (Piper 1944). A Piper diagram is used to categories the hydrochemical facies involved in controlling the groundwater chemistry.

### Rock–water interaction

The rock–water interaction which governs the groundwater chemistry can be better understood by comparing the concentration of TDS versus  $(Na^+ + K^+) / (Na^+ + K^+ + Cl^-)$  and TDS versus  $Cl^- / (Cl^- + HCO_3^-)$  using Gibbs’ plots (Gibbs 1970). Gibbs’ plot has three major categories viz., precipitation, rock, and evaporation dominance. This plot has been widely used in discriminating groundwater chemistry. Gibbs’ ratios were estimated by following equations, where all ionic measurements are in meq/l.

$$\text{Gibb's ratio I} = (Na^+ + K^+) / (Na^+ + K^+ + Ca^{+2}) \tag{5}$$

$$\text{Gibb's ratio II} = Cl^- / (Cl^- + HCO_3^-) \tag{6}$$

### Principal component analyses (PCA)

The principal component analysis (PCA) provides a single resolution and reconstruction of novel outcomes for a large

**Table 1** Statistical summary of major ions concentrations of groundwater for pre- and post-rainfall seasons

| Parameters                    | Pre-rainfall season |         |         |         |                                   | Post-rainfall season |         |         |         |                                   |                             |
|-------------------------------|---------------------|---------|---------|---------|-----------------------------------|----------------------|---------|---------|---------|-----------------------------------|-----------------------------|
|                               | Min                 | Max     | Ave     | SD      | % of samples exceeding the limits | Min                  | Max     | Ave     | SD      | % of samples exceeding the limits | BIS (2012) Acceptable limit |
| pH                            | 6.70                | 8.10    | 7.30    | 0.27    | –                                 | 6.80                 | 8.0     | 7.24    | 0.26    | –                                 | 6.5–8.5                     |
| EC                            | 314.06              | 5643.75 | 1947.97 | 1460.61 | –                                 | 240.63               | 5401.56 | 1977.21 | 1456.30 | –                                 | 750                         |
| TDS                           | 201.0               | 3612.0  | 1246.70 | 934.79  | 84                                | 154.0                | 3457.0  | 1265.42 | 937.78  | 78                                | 500                         |
| Ca <sup>2+</sup>              | 28.0                | 203.57  | 95.16   | 45.19   | 66                                | 3.0                  | 541.35  | 107.29  | 81.68   | 68                                | 75                          |
| Mg <sup>2+</sup>              | 7.40                | 127.44  | 56.53   | 32.48   | 42                                | 7.63                 | 193.81  | 67.17   | 43.46   | 54                                | 50                          |
| Na <sup>+</sup>               | 15.98               | 534.96  | 149.42  | 142.05  | 24                                | 7.05                 | 476.31  | 135.33  | 126.78  | 32                                | 200                         |
| K <sup>+</sup>                | 1.10                | 85.92   | 10.61   | 16.85   | 20                                | 1.0                  | 103.51  | 10.47   | 19.53   | 16                                | 12                          |
| HCO <sub>3</sub> <sup>-</sup> | 124.44              | 758.84  | 409.72  | 132.49  | 84                                | 43.92                | 630.0   | 194.66  | 128.99  | 32                                | 300                         |
| Cl <sup>-</sup>               | 7.81                | 1667.46 | 354.67  | 453.67  | 38                                | 7.63                 | 1089.20 | 256.69  | 274.13  | 38                                | 250                         |
| SO <sub>4</sub> <sup>2-</sup> | 0.0                 | 1533.03 | 162.21  | 296.92  | 24                                | 5.18                 | 1200.0  | 146.34  | 237.05  | 22                                | 200                         |
| NO <sub>3</sub> <sup>-</sup>  | 0.09                | 897.28  | 123.65  | 151.45  | 62                                | 0.0                  | 606.10  | 120.30  | 133.10  | 64                                | 45                          |
| F <sup>-</sup>                | 0.28                | 5.48    | 1.18    | 0.89    | 32                                | 0.21                 | 4.43    | 1.35    | 0.95    | 30                                | 1.5                         |

all values are in mg/l except EC and pH; EC unit is µS/cm  
 Min, minimum; Max, maximum; Ave, average; SD, standard deviation

**Table 2** Key parameters for computing the exposure risk of F<sup>-</sup> and NO<sub>3</sub><sup>-</sup> through ingestion and dermal pathways

| Parameters                                  | Unit              | 6–12 months   | 6–11 years | 11–16 years | 16–18 years | 18–21 years | ≥ 21 years | > 65 years |
|---|-------------------|---------------|------------|-------------|-------------|-------------|------------|------------|
| <b>Ingestion pathway</b>                    |                   |               |            |             |             |             |            |            |
| Ingestion rate (IR <sub>w</sub> )           | L/day             | 1             | 1.32       | 1.82        | 1.78        | 2.34        | 2.94       | 2.73       |
| Exposure frequency (E <sub>fr</sub> )       | Days/year         | 365           | 365        | 365         | 365         | 365         | 365        | 365        |
| Exposure duration (ED)                      | Year              | 6             | 6          | 6           | 6           | 30          | 30         | 30         |
| Body Weight (BW)                            | kg                | 9.1           | 29.3       | 54.2        | 67.6        | 67.6        | 78.8       | 80         |
| Average time (AT <sub>r</sub> )             | Days              | 2190          | 2190       | 2190        | 2190        | 10,950      | 10,950     | 10,950     |
| Concentration of element (C <sub>fw</sub> ) | mg/l              | Present study |            |             |             |             |            |            |
| <b>Dermal pathway</b>                       |                   |               |            |             |             |             |            |            |
| Skin surface area (SA)                      | cm <sup>2</sup>   | 4500          | 10,500     | 15,700      | 18,000      | 19,550      | 19,800     | 19,400     |
| Exposure time (ET)                          | h/event           | 0.54          | 0.54       | 0.54        | 0.54        | 0.71        | 0.71       | 0.71       |
| Exposure frequency (E <sub>fr</sub> )       | days/year         | 350           | 350        | 350         | 350         | 350         | 350        | 350        |
| Exposure duration (ED)                      | year              | 6             | 6          | 6           | 6           | 30          | 30         | 30         |
| Conversion factor (CF)                      | l/cm <sup>3</sup> | 0.001         | 0.001      | 0.001       | 0.001       | 0.001       | 0.001      | 0.001      |
| Body weight (BW)                            | kg                | 9.1           | 29.3       | 54.2        | 67.6        | 67.6        | 78.8       | 80         |
| Average time (AT <sub>r</sub> )             | days              | 2190          | 2190       | 2190        | 2190        | 2190        | 2190       | 2190       |
| Skin adherence factor (K <sub>p</sub> )     | cm/h              | 0.001         | 0.001      | 0.001       | 0.001       | 0.001       | 0.001      | 0.001      |
| Concentration of element (C <sub>fw</sub> ) | mg/l              | Present study |            |             |             |             |            |            |

dataset (Li et al. 2019b). The principal components (PCs) were taken out of the varimax rotation of loadings for the extreme variance and eigenvalues. PCA was done by considering all ions and various groups of these ions in terms of PCs which can give information on the geochemical processes as well as the sources and origin of the poorer quality of water.

**Health risk assessment**

Hazard quotient (HQ) through ingestion (HQ<sub>ing</sub>) and dermal (HQ<sub>der</sub>) for F<sup>-</sup> and NO<sub>3</sub><sup>-</sup> ions for various age groups were estimated by following the guidelines of the United States Environmental Protection Agency’s Exposure Factor Handbook (U.S. EPA 2011) for pre- and post-rainfall seasons. Chronic daily dose and hazard quotient of F<sup>-</sup> and NO<sub>3</sub><sup>-</sup> via ingestion (HQ<sub>ing</sub>) and dermal (HQ<sub>der</sub>) pathways are calculated using the below equations:

$$CDD_{ing} = \frac{C_{fw} \times IR_w \times E_{fr} \times ED}{BW \times AT} \tag{7}$$

$$CDD_{der} = \frac{C_{fw} \times ESA \times K \times E_{fr} \times ED \times CF}{BW \times AT} \tag{8}$$

$$HQ_{ing} = \frac{CDD_{ing}}{RfD} \tag{9}$$

$$HQ_{der} = \frac{CDD_{der}}{RfD} \tag{10}$$

“CDD<sub>ing</sub> indicates chronic exposure dosage (daily) through ingestion pathway (mg/kg/day), CDD<sub>der</sub> indicates chronic

exposure dosage (daily) through the dermal pathway (mg/kg day), C<sub>fw</sub> indicates F<sup>-</sup> and NO<sub>3</sub><sup>-</sup> content in a sample (mg/l), E<sub>fr</sub> indicates rate of exposure (days/years), ED indicates exposure period (years), BW indicates body weight (kg), AT indicates average period (days/years), ESA indicates exposed skin area (cm<sup>2</sup>), K indicates skin adherence factor, CF indicates conversion factor (l/cm<sup>3</sup>), and RfD indicates reference quantity of F<sup>-</sup> and NO<sub>3</sub><sup>-</sup> (0.06 and 1.6 mg/kg/day)”. These parameter values for calculating the risk of F<sup>-</sup> and NO<sub>3</sub><sup>-</sup> through different pathways are presented in Table 2.

**Results and discussion**

**Groundwater characteristics**

The pH ranged from 6.70 to 8.10 and 6.80 to 8.0 with an average of 7.30 and 7.24 for the pre- and post-rainfall seasons, respectively (Table 1), which specifies that water is slightly neutral to alkaline in nature. All the water samples are within the permissible limit of drinking standards (BIS 2012). TDS ranged from 201 to 3612 mg/l and 154 to 3457 mg/l with a mean value of 1246.70 mg/l and 1265.42 mg/l for pre- and post-rainfall seasons respectively (Table 1). Around 84% and 78% of the samples exceed the drinking water limit of 500 mg/l for pre- and post-rainfall season which causes gastrointestinal irritation (BIS 2012). The spatial distribution map of TDS for both seasons is shown in Fig. 3.

## Cations

The  $\text{Ca}^{2+}$  content ranged from 28 to 203.57 mg/l and 3.0 to 541.35 mg/l with mean values of 95.16 mg/l and 107.29 mg/l for pre- and post-rainfall season (Table 1).  $\text{Ca}^{2+}$  has a permissible limit of 75 mg/l and about 66% and 68% of the sample from pre- and post-rainfall seasons are exceeding the permissible limit respectively (BIS 2012). The main source of  $\text{Ca}^{2+}$  in water is mainly because of the deterioration and dissolution of plagioclase feldspar minerals (Marghade et al. 2021). The  $\text{Mg}^{2+}$  ranged between 7.40 and 127.44 mg/l and 7.63 and 193.81 mg/l with a mean value of 56.53 mg/l and 67.17 mg/l for pre- and post-rainfall season, respectively (Table 1). Around 42% and 54% of samples exceeded the tolerable limit of 50 mg/l for pre- and post-rainfall seasons (BIS 2012).  $\text{Mg}^{2+}$  is largely accredited for the dissolution of ferromagnesian minerals like olivine, pyroxene, and biotite, existing in the host rocks, and human-induced actions (Subba Rao 2021).  $\text{Na}^+$  ranged from 15.98 to 534.96 mg/l and 7.05 to 476.31 mg/l with an average of 149.42 mg/l and 135.33 mg/l for pre- and post-rainfall season (Table 1). Only 24% and 22% of samples show  $\text{Na}^+$  more than the prescribed limit (200 mg/l) for pre- and post-rainfall seasons (BIS 2012). Minerals like plagioclase feldspars in the host rocks, household waste, and irrigation return flow are the prime anthropogenic sources for elevated  $\text{Na}^+$  concentration in water (Subba Rao 2021).  $\text{K}^+$  ranged from 1.10 to 85.92 mg/l and 1.0 to 103.51 mg/l with an average of 10.61 mg/l and 10.47 mg/l for pre- and post-rainfall season (Table 1). Around 20%

and 16% of the samples for pre- and post-rainfall season exceed the permissible limit (12 mg/l). The primary origin of elevated  $\text{K}^+$  content in water is due to the presence of Orthoclase feldspars minerals and potassium composts.

## Anions

$\text{HCO}_3^-$  Ranged from 124.44 to 758.84 mg/l and 43.92 to 630 mg/l with mean value of 409.72 mg/l and 194.66 mg/l for pre- and post-rainfall season (Table 1). The elevated  $\text{HCO}_3^-$  concentration was due to the release of  $\text{CO}_2$  gases from the decomposition of organic decay. Around 84% and 32% of samples of pre- and post-rainfall seasons, respectively, are beyond the permissible limit (BIS 2012). The  $\text{Cl}^-$  concentration ranged from 7.81 to 1667.46 mg/l and 7.63 to 1089.20 mg/l with mean values of 354.67 mg/l and 256.69 mg/l (Table 1).  $\text{Cl}^-$  concentration is more than 250 mg/l in 38% of samples for pre- and post-rainfall seasons (Table 1). A high content of  $\text{Cl}^-$  causes a salty taste and laxative effect. Domestic wastewater, return irrigation flow, etc., are the prime sources of high concentration of  $\text{Cl}^-$  in water (Laxmankumar et al. 2019).  $\text{SO}_4^{2-}$  values range from 0 to 1533.03 mg/l and 5.18 to 1200 mg/l with an average of 162.21 mg/l and 146.34 mg/l for pre- and post-rainfall seasons (Table 1). Around 24% and 22% of water samples for pre- and post-rainfall seasons are above the permissible limit of 200 mg/l (BIS 2012). Various farming practices and the excess use of fertilizers to increase soil permeability may be a source of elevated concentration (Katla et al. 2021).

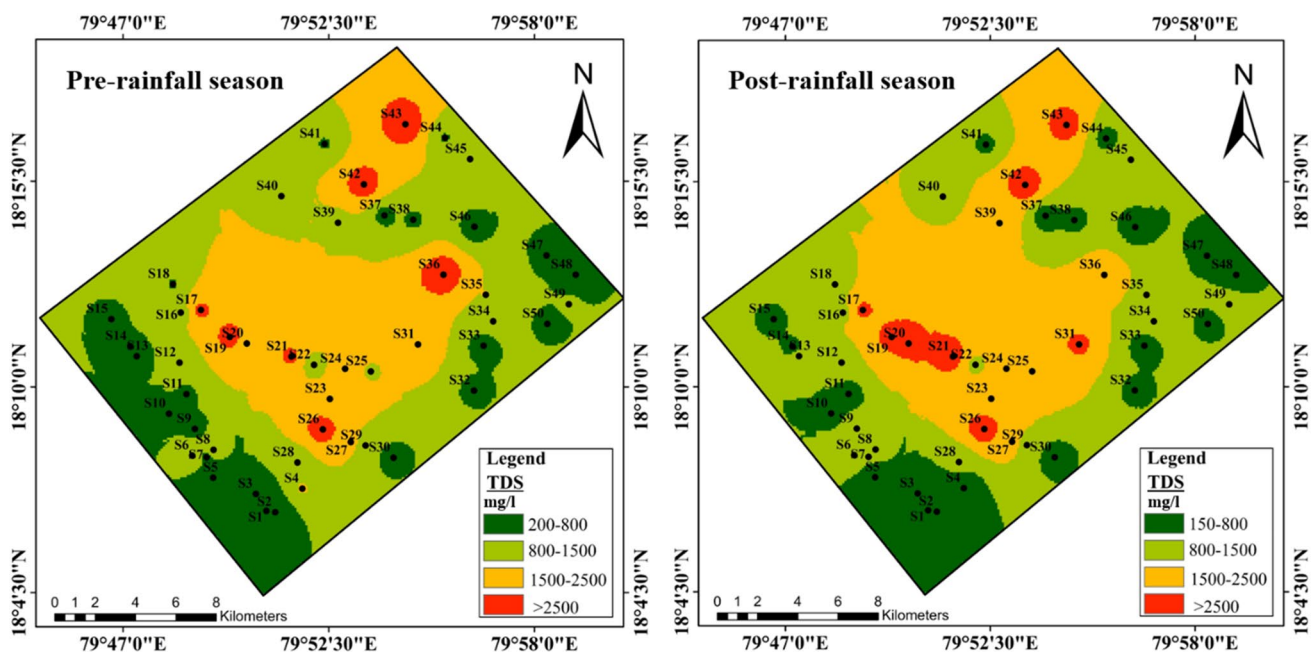


**Fig. 3** Spatial distribution map of TDS concentration (mg/l) for pre- and post-rainfall seasons

### Fluoride and nitrate

F<sup>-</sup> concentration was ranged between 0.28 and 5.48 mg/l and 0.21 and 4.43 mg/l with an average of 1.18 mg/l and 1.35 mg/l for pre- and post-rainfall seasons (Table 1). Around 32% and 30% of samples for pre- and post-rainfall seasons exceeds the desirable limit of 1.5 mg/l (BIS 2012). The excess F<sup>-</sup> content in water causes fluorosis and its sources are due to the presence of granitic rock in the area which is rich in fluoride bearing minerals like biotite, fluorite, and hornblende. Also, the dolomite and conglomerate rock in the area leading to the dissolution of calcium-bearing minerals like fluorite can increase fluoride concentration in groundwater (Kechiched et al 2020). The spatial distribution of F<sup>-</sup> concentration for pre- and the post-rainfall seasons is shown in Fig. 4. The southwestern, central, and few patches in the northern and eastern part shows high fluoride content for both the seasons.

Similarly, the NO<sub>3</sub><sup>-</sup> concentration ranged from 0.09 to 897.28 mg/l and 0 to 606.10 mg/l with an average of 123.65 mg/l and 120.30 mg/l for pre- and post-rainfall seasons (Table 1). Elevated NO<sub>3</sub><sup>-</sup> concentration was observed in 62% and 64% of samples beyond its permissible limit of 45 mg/l (BIS 2012). The excess of NO<sub>3</sub><sup>-</sup> concentration in water causes a disease called a blue baby syndrome. Sewage waste effects, seepages from the septic tank, and surplus uses of animal waste and fertilizers exceeds the NO<sub>3</sub><sup>-</sup> content in water (Gugulothu 2022a). The permissible limit of NO<sub>3</sub><sup>-</sup> was observed in patches at a few places, while the remaining area shows a high concentration. The distribution

of high NO<sub>3</sub><sup>-</sup> content is observed in the southwestern, and central parts of the area for pre- and post-rainfall seasons is shown in Fig. 5. The high NO<sub>3</sub><sup>-</sup> content part falls in the cropland area where agricultural practices like excessive use of fertilizer lead to elevation of NO<sub>3</sub><sup>-</sup> in groundwater (Subba Rao et al. 2020).

The F<sup>-</sup> and NO<sub>3</sub><sup>-</sup> concentrations in semi-arid regions of Telangana State was compared and found that the F<sup>-</sup> concentration was similar in range with other studies, while the NO<sub>3</sub><sup>-</sup> concentration was higher in present study as compare to other semi-arid regions of India and worldwide. The comparative values of F<sup>-</sup> and NO<sub>3</sub><sup>-</sup> are given in Table 3.

The F<sup>-</sup> concentration in groundwater was divided into three different categories viz., Category-1 (concentration ≤ 0.5 mg/l), Category-2 (concentration > 0.5 to ≤ 1.5 mg/l), and Category-3 (concentration > 1.5 mg/l) (Table 4). The F<sup>-</sup> content in Category-1 has 20% of samples for both seasons and ingestion of such water may cause dental caries. Category-2 has 48% and 44% of samples from pre- and post-rainfall seasons, respectively, and is fit for drinking purposes, while Category-3 has 32% and 36% of samples from pre- and post-rainfall seasons and is unfit for drinking purposes (Table 4 and Fig. 6). Intake of such high F<sup>-</sup> content water may lead to dental and skeletal fluorosis (Ali et al. 2019). Similarly, NO<sub>3</sub><sup>-</sup> concentration in groundwater was also divided into three categories. Category-1 (concentration ≤ 45 mg/l), Category-2 (concentration > 45 to ≤ 100 mg/l), and Category-3 (concentration > 100 mg/l) (Table 4). The NO<sub>3</sub><sup>-</sup> content in Category-1 has 38% and 36% of samples for pre- and

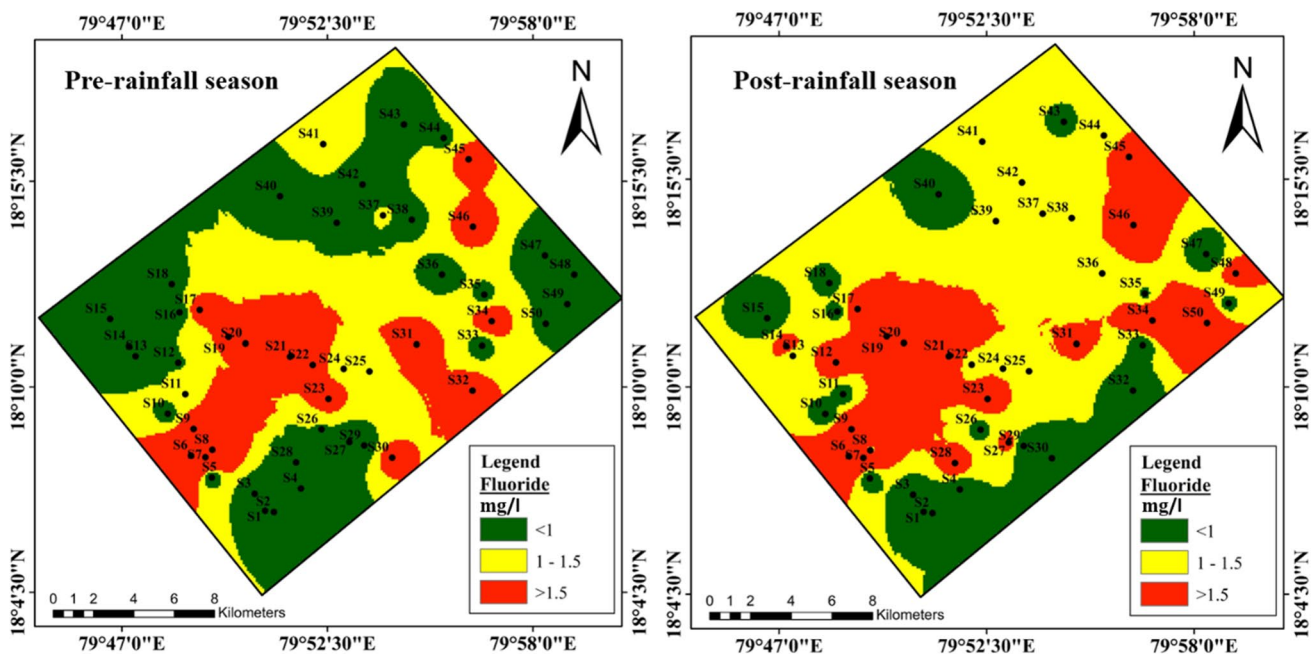


Fig. 4 Spatial distribution map of F<sup>-</sup> concentration (mg/l) for pre- and post-rainfall seasons



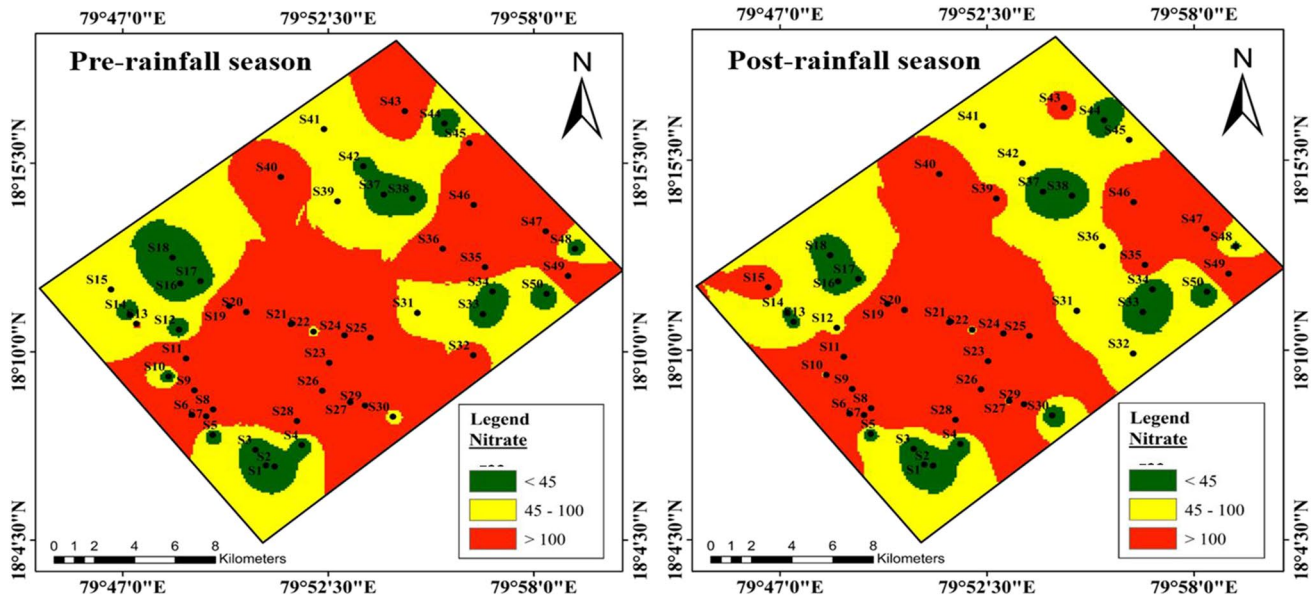


Fig. 5 Spatial distribution map of NO<sub>3</sub><sup>-</sup> concentration (mg/l) for pre- and post-rainfall seasons

post-rainfall seasons and are fit for drinking and irrigation uses. Category-2 has 12% and 20% of samples, and Category-3 has 50% and 44% of samples and is unfit for irrigation and drinking purposes (Table 4 and Fig. 6).

**Water quality index for drinking purpose**

Water quality index (WQI) is a gauge to quantify the drinking water standard (Subba Rao et al. 2020). The calculated WQI ranged from 18.3 to 233 and 12.97 to 219.14

for pre- and post-rainfall seasons. According to the classification of WQI, 12 and 14 samples have WQI ≤ 50 and 24% and 28% of samples show excellent water quality for pre- and post-rainfall seasons and are fit for drinking purposes (Table 5). WQI ≥ 50 ≤ 100 shows 22% and 44% of samples shows good water quality for pre- and post-rainfall seasons (Table5). WQI ≥ 100 ≤ 200 shows 10 and 11 samples with 20% and 22% shows poor water quality and WQI ≥ 200 ≤ 300; 6 and 3 samples with 12% and 6% shows very poor water for pre- and post-rainfall seasons (Table 5).

**Table 3** Comparative study of F<sup>-</sup> and NO<sub>3</sub><sup>-</sup> concentration (mg/l) in groundwater studies of India and worldwide

| Study area/region   | F <sup>-</sup> (mg/l) |        | NO <sub>3</sub> <sup>-</sup> (mg/l) |          | References                 |
|---------------------|-----------------------|--------|-------------------------------------|----------|----------------------------|
|                     | Range                 | Mean   | Range                               | Mean     |                            |
| South India         | 0.84–4.3              | 1.95   | 2.2–165                             | 55.61    | Adimalla et al. (2020)     |
| Rural Telangana     | 0.22–5.41             | 1.13   | 0.04–585                            | 56.3     | Goguluthu et al. (2022a)   |
| Maheshwaram         | 0.31–3.30*            | 1.44*  | 3–200*                              | 62.09*   | Laxman Kumar et al. (2019) |
|                     | 0.28–2.58**           | 1.20** | 4–128**                             | 46.91**  |                            |
| Suryapeth           | 0.11–1.71*            | 0.77*  | 13–125*                             | 51.36*   | Katla et al. (2021)        |
|                     | 0.31–1.64**           | 0.66** | 13–176**                            | 94.55**  |                            |
| Yadadri-Bhuvanagiri | 0.43–2.93*            | 1.53*  | 8.26–394.53*                        | 74.17*   | More et al. (2021)         |
|                     | 0.60–3.56**           | 1.72** | 0.0–506.67**                        | 79.09**  |                            |
| Chinnakodur         | 0.50–3.50             | -      | 12–212                              | -        | Adimalla and Li (2019)     |
| China               | 0.11–6.33             |        | 2.66–103                            |          | Chen et al. (2017b)        |
| North China         | 0.03–9.42             | 0.55   | -                                   | -        | Yuan et al. 2020           |
| Pakistan            | -                     | -      | 0.1–1.1                             | 0.389    | Rehman et al. (2020)       |
| Turkey              | -                     | -      | 23–296***                           | 117***   | Ustaoğlu and Tepe (2019)   |
| Iran                | 0.27–10.3             | 1.70   | -                                   | -        | Yousefi et al. 2018        |
| Present study       | 0.28–5.48*            | 1.18*  | 0.09–897.28*                        | 123.65*  | -                          |
|                     | 0.21–4.43**           | 1.35** | 0.0–606.10**                        | 120.30** |                            |

\*pre-rainfall, \*\*post-rainfall, and \*\*\*sediment sample

**Table 4** Different categories of F<sup>-</sup> and NO<sub>3</sub><sup>-</sup> concentration in groundwater for pre- and post-rainfall seasons

| Category   | F <sup>-</sup> Conc (mg/l) | Pre-rainfall   |              | Post-rainfall  |              | NO <sub>3</sub> <sup>-</sup> Conc (mg/l) | Pre-rainfall   |              | Post-rainfall  |              |
|------------|----------------------------|----------------|--------------|----------------|--------------|--|----------------|--------------|----------------|--------------|
|            |                            | No. of Samples | % of Samples | No. of Samples | % of Samples |  | No. of Samples | % of Samples | No. of Samples | % of Samples |
| Category-1 | F <sup>-</sup> ≤ 0.5       | 10             | 20           | 10             | 20           | NO <sub>3</sub> <sup>-</sup> ≤ 45        | 19             | 38           | 18             | 36           |
| Category-2 | F <sup>-</sup> > 0.5 ≤ 1.5 | 24             | 48           | 22             | 44           | NO <sub>3</sub> <sup>-</sup> > 45 ≤ 100  | 6              | 12           | 10             | 20           |
| Category-3 | F <sup>-</sup> > 1.5       | 16             | 32           | 18             | 36           | NO <sub>3</sub> <sup>-</sup> > 100       | 25             | 50           | 22             | 44           |

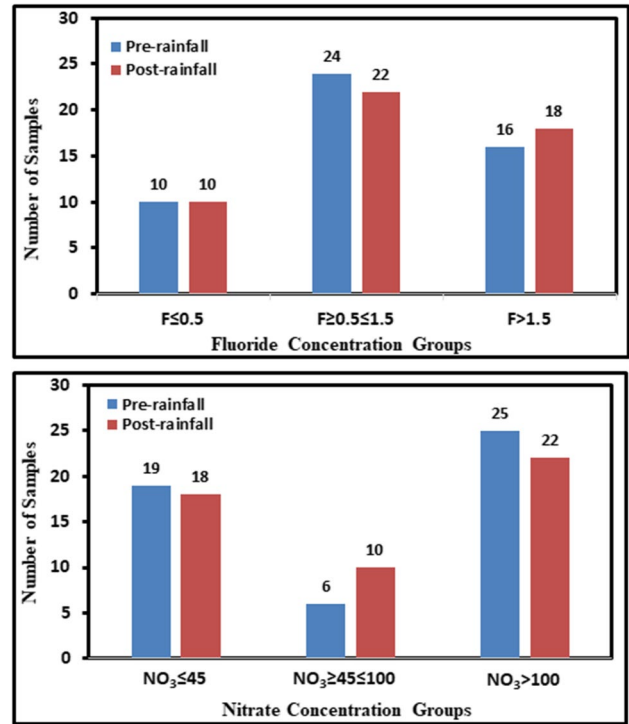


**Fig. 6** Different groups of F<sup>-</sup> and NO<sub>3</sub><sup>-</sup> concentrations (mg/l) for pre- and post-rainfall seasons

No samples show unsuitability for drinking purpose, and the distribution map of WQI for both seasons is shown in Fig. 7.

### Geochemical evolution

Geochemical evolution of the water quality concerning ion's dominance, Piper trilinear diagram was widely accepted and used (Piper 1944). From the Piper diagram, it is detected that 46% and 51% of the water samples for pre- and post-rainfall seasons represents carbonate water type (Ca<sup>2+</sup>.HCO<sub>3</sub><sup>-</sup>), and 4% of each water sample show non-carbonate water type (Ca<sup>2+</sup>.Cl<sup>-</sup>), 12% of each water samples are non-alkali water type (Na<sup>+</sup>.Cl<sup>-</sup>), 32% and 28% water samples show (Ca<sup>2+</sup>.Na<sup>+</sup>.HCO<sub>3</sub><sup>-</sup>) type water, and 6% and 5% show mixed water type (Ca<sup>2+</sup>.Mg<sup>2+</sup>.Cl<sup>-</sup>) for pre- and post-rainfall seasons (Fig. 8). The dominance of the carbonate water types over alkaline earth (Ca<sup>2+</sup> and Mg<sup>2+</sup>) and weak acids (HCO<sub>3</sub><sup>-</sup>) are significantly higher than the alkalis (Na<sup>+</sup> and K<sup>+</sup>) and strong acids (Cl<sup>-</sup> and SO<sub>4</sub><sup>2-</sup>), representing the prevailing conditions of the water–rock interactions (Gugulothu 2022b). The mixed type water with the dominance of (Ca<sup>2+</sup>.Mg<sup>2+</sup>.Cl<sup>-</sup>) ions and excess type water with (Na<sup>+</sup>.Cl<sup>-</sup>) dominance and (Ca<sup>2+</sup>.Mg<sup>2+</sup>.Cl<sup>-</sup>) type water signifies the movement of the carbonate type towards the mixed type water and excess type water, which also evidently agrees with the control of water–rock interactions in the aquifer regime. Further, the geochemical evolution of the

**Table 5** Classification of the WQI scores for pre- and post-rainfall seasons

| WQI range   | Type of water           | Pre-rainfall ( <i>n</i> = 50) |              | Post-rainfall ( <i>n</i> = 50) |              |
|-------------|-------------------------|-------------------------------|--------------|--------------------------------|--------------|
|             |                         | No. of samples                | % of samples | No. of samples                 | % of samples |
| ≤ 50        | Excellent water         | 12                            | 24           | 14                             | 28           |
| > 50 ≤ 100  | Good water              | 22                            | 44           | 22                             | 44           |
| > 100 ≤ 200 | Poor water              | 10                            | 20           | 11                             | 22           |
| > 200 ≤ 300 | Very poor water         | 06                            | 12           | 03                             | 06           |
| > 300       | Unsuitable for drinking | Nil                           | Nil          | Nil                            | Nil          |

water types is in descending order of carbonate water > mixed water > non-alkali water.

### Rock–water interaction (Gibbs' plot)

Pre- and post-rainfall chemical analyzed data of the water sample was plotted on the Gibbs' plot showing the three important controlling mechanisms of the water chemistry. The three major mechanism processes are precipitation, rock, and evaporation dominance (Gibbs 1970). The plots are the fraction of cations  $[(Na^+ + K^+) / (Na^+ + K^+ + Ca^{2+})]$  and anions  $[Cl^- / (Cl^- + HCO_3^-)]$  in contrast to TDS. The plots suggest the majority of the samples for pre- and post-rainfall seasons were categorized in the evaporation mechanism with few samples are of rock mechanism (Fig. 9a and b). The evaporation mechanism was due to an increase of  $Cl^-$  and  $Na^+$  ions which increases the TDS, while rock mechanism samples depend on the factors like arid conditions of the region, low rainfall, high temperature, and residence period in the aquifer.

### Principal component analyses (PCA)

To decrease the dimensionality space of the larger dataset into smaller clustering, principal component analysis (PCA) was used. A factor analysis was performed on the varimax normalized data to identify the factors influencing the compositional patterns between the analyzed water samples. The factor loading into three categories: strong, moderate, and weak, with absolute loading values of > 0.70, 0.50–0.30, and 0.50–0.30, respectively. A total of 12 parameters are explained. PCA revealed those three and four components which explains 74.85% and 79.30% of the total variance for pre- and post-rainfall seasons (Table 6). In the pre-rainfall season, PC1 represents 48.60% of the variance with strong positive loadings on EC, TDS,  $Ca^{2+}$ ,  $Na^+$ ,  $Mg^{2+}$ ,  $K^+$ ,  $SO_4^{2-}$ ,  $Cl^-$ , and  $HCO_3^-$  due to mineral weathering and water–rock interactions. PC2 represents 13.48% of the total variance and had high  $NO_3^-$  loadings and negative  $CO_3^{2-}$ ,  $K^+$  loadings, indicating ion exchange and carbonate weathering, as well as anthropogenic influences. PC3 represents 12.77% of the

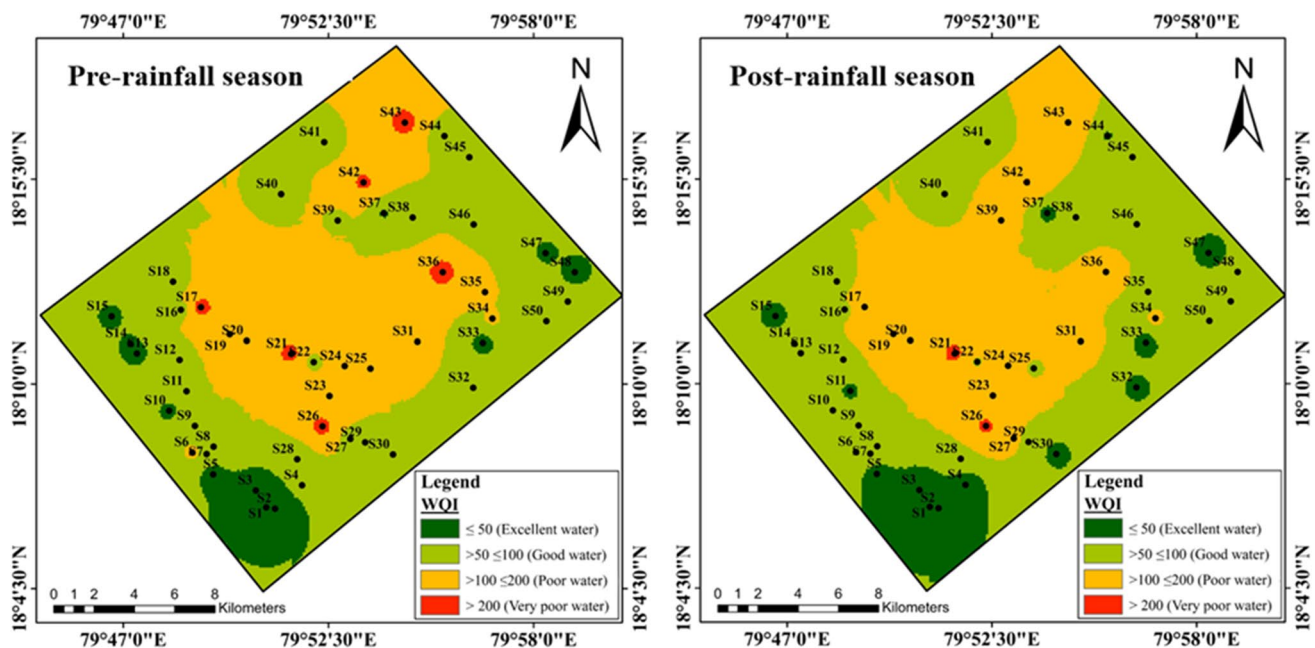
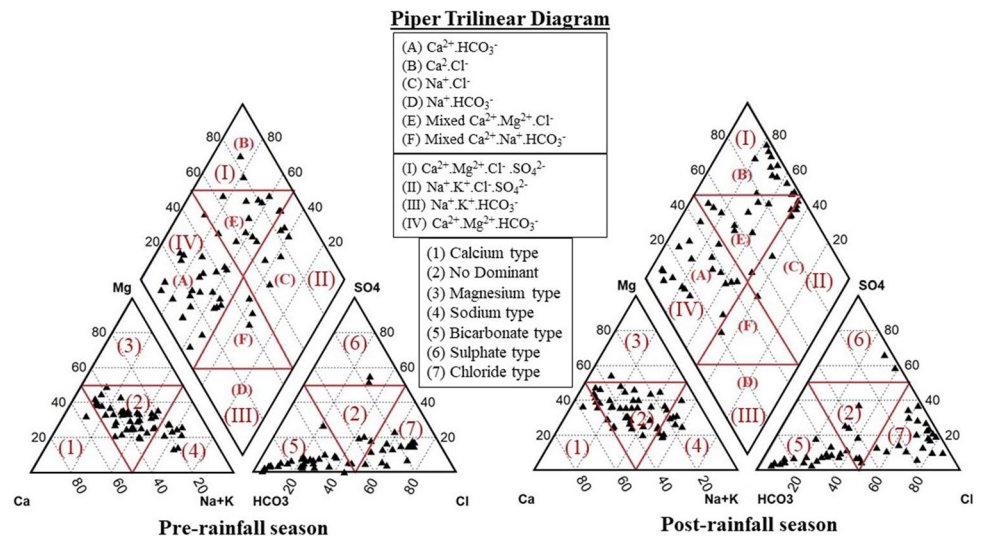


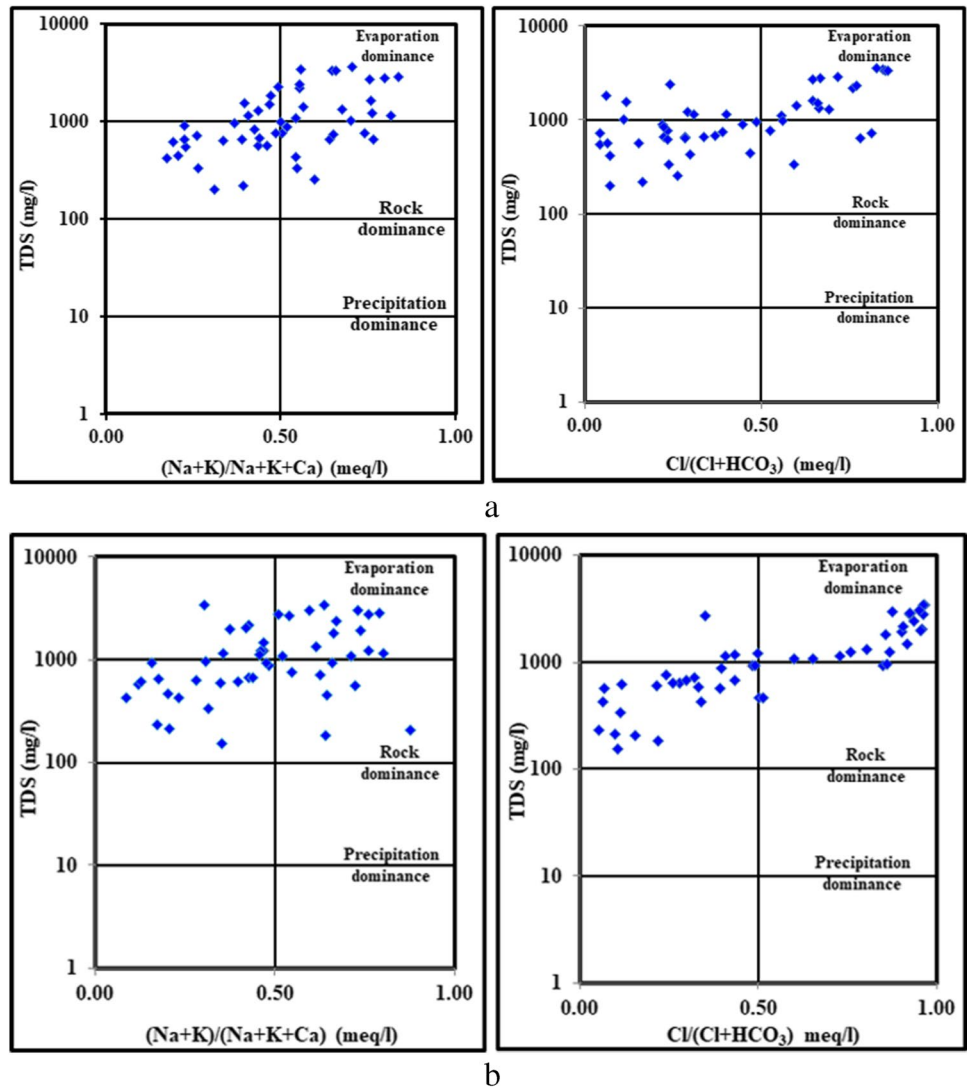
**Fig. 7** Spatial distribution of water quality index (WQI) for pre- and post-rainfall seasons

**Fig. 8** Piper diagram showing water facies for pre- and post-rainfall seasons



total variance and has high loadings on  $\text{F}^-$ , pH, and  $\text{Ca}^{2+}$  loading, which indicates weathering reactions involving

**Fig. 9** (a) Gibbs plot for pre-rainfall season. (b) Gibbs plot for post-rainfall season



fluoride-bearing minerals (apatite, hornblende, mica, etc.).

As a result of the four-principal component analysis, 79.30% of the total cumulative percentages in the post-rainfall season were explained, and components PC1, PC2, PC3, and PC4 were found to contribute to the variations in groundwater quality, accounting for 39.89%, 20.05.9%, 9.60%, and 9.23% of the total variance. PC1 shows high positive loadings on  $\text{Na}^+$ ,  $\text{SO}_4^{2-}$ , EC, TDS,  $\text{Cl}^-$ ,  $\text{K}^+$ , and  $\text{Mg}^{2+}$ . As a result of high  $\text{NO}_3^-$  loadings in areas where a great deal of fertilizer has been applied, PC2 has significant positive loadings on  $\text{NO}_3^-$ ,  $\text{Ca}^{2+}$ ,  $\text{Mg}^{2+}$ , and  $\text{Cl}^-$ , but negative loadings on  $\text{CO}_3^-$ , indicating a predominant process of ion exchange and carbonate weathering and leaching from fluoride-rich minerals. PC3 had strong positive loadings on  $\text{F}^-$  and  $\text{HCO}_3^-$ . PC4 had strong positive loadings on pH. The principal component plot in rotated space for pre- and post-rainfall seasons is shown in Fig. 10a. The grouping of these ions with TDS reproduces the salinity in water indicating the main cause of anthropogenic and human interference contamination in the aquifer regime (Dhakate et al. 2013; Ustaoğlu and Tepe 2019; Aydin et al. 2021). This group and positive loading of  $\text{F}^-$  influences the dissolution and weathering of fluoride being minerals presenting in the rocks rather than the uses of fertilizers (Subba Rao et al. 2020). The role of PCA supports the geogenic and anthropogenic activities for variation of water chemical quality.

Cluster analysis (CA) is a linkage used to determine the major ions from the analyzed groundwater samples and grouping for clustering of the Euclidean distance from Ward's method by using software of SPSS version 23. CA is a totally

linkage used to determine the distance between the clusters by the greatest between the examples, as it is a geometric distance in a multi-dimensional space. A graphical representation of the hierarchical clustering or grouping along with the corresponding distance to achieve a linkage is called dendrogram. The CA of chemical variables gives information on geochemical processes controlling the groundwater chemistry, while the group analysis of groundwater sampling sites provides the information, where the geochemical processes cause the variation of groundwater contamination.

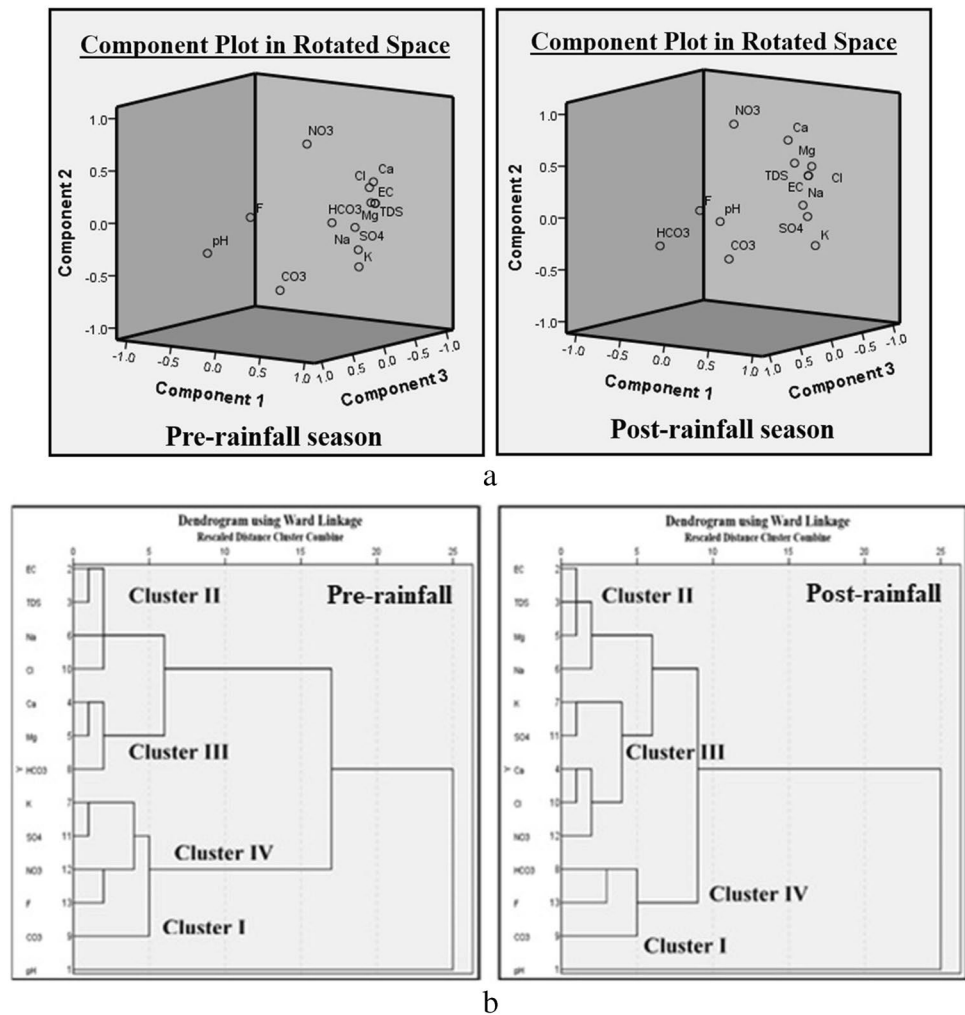
The results of CA of chemical variables (pH, TDS, TH,  $\text{Ca}^{2+}$ ,  $\text{Mg}^{2+}$ ,  $\text{Na}^+$ ,  $\text{K}^+$ ,  $\text{HCO}_3^-$ ,  $\text{Cl}^-$ ,  $\text{SO}_4^{2-}$ , and  $\text{NO}_3^-$ ) are presented in a dendrogram (Fig. 10b). According to the dendrogram, Clusters I, II, III, and IV have a linkage distance of 5 to 25. Pre-rainfall season pH is measured by Cluster I; EC, TDS,  $\text{Na}^+$ , and  $\text{Cl}^-$  are measured as Cluster II;  $\text{Ca}^{2+}$ ,  $\text{Mg}^{2+}$ , and  $\text{HCO}_3^-$  are measured by Cluster III; and  $\text{K}^+$ ,  $\text{SO}_4^{2-}$ ,  $\text{NO}_3^-$ , and  $\text{F}^-$  are measured by Cluster IV (Fig. 10b). In the post-rainfall season, CA is used to measure variables from Cluster I pH; Cluster II represents EC, TDS,  $\text{Mg}^{2+}$ , and  $\text{Na}^+$ ; Cluster III represents  $\text{K}^+$ ,  $\text{SO}_4^{2-}$ ,  $\text{Ca}^{2+}$ ,  $\text{Cl}^-$ , and  $\text{NO}_3^-$ ; and Cluster IV represents  $\text{HCO}_3^-$ ,  $\text{F}^-$ , and  $\text{CO}_3^-$  (Fig. 10b). The overall cluster analysis indicates that pre- and post-rainfall seasons display predominant ion exchange, silicate group minerals of weathering, salinization of the water, and a high value of  $\text{NO}_3^-$  concentration, resulting from fertilizers used in irrigation and fluoride-rich minerals (Subba Rao et al. 2020).

**Table 6** Principal component analysis for groundwater samples during pre- and post-rainfall seasons

| Parameters               | Principal component analysis for groundwater samples |              |              |                       |              |              |              |
|--------------------------|--|--------------|--------------|-----------------------|--------------|--------------|--------------|
|                          | Pre-rainfall season                                  |              |              | Post-rainfall seasons |              |              |              |
|                          | PC1  | PC2          | PC3          | PC1                   | PC2          | PC3          | PC4          |
| pH                       | -0.346   | -0.260       | <b>0.747</b> | -0.063                | -0.073       | 0.111        | <b>0.909</b> |
| EC                       | <b>0.918</b>   | 0.217        | -0.135       | <b>0.855</b>          | 0.448        | 0.004        | -0.110       |
| TDS                      | <b>0.918</b>   | 0.217        | -0.135       | <b>0.855</b>          | 0.448        | 0.004        | -0.110       |
| $\text{Ca}^{2+}$         | <b>0.738</b>   | 0.371        | -0.366       | 0.472                 | <b>0.720</b> | -0.216       | -0.171       |
| $\text{Mg}^{2+}$         | <b>0.908</b>   | 0.229        | -0.085       | <b>0.722</b>          | 0.560        | 0.037        | -0.041       |
| $\text{Na}^+$            | <b>0.924</b>   | 0.035        | 0.194        | <b>0.918</b>          | 0.195        | 0.180        | 0.103        |
| $\text{K}^+$             | 0.637  | -0.438       | -0.277       | <b>0.749</b>          | -0.275       | -0.261       | 0.049        |
| $\text{HCO}_3^-$         | 0.623  | 0.040        | 0.134        | -0.410                | -0.273       | 0.595        | -0.350       |
| $\text{Cl}^-$            | <b>0.799</b>   | 0.344        | -0.215       | <b>0.754</b>          | 0.499        | -0.195       | -0.007       |
| $\text{SO}_4^{2-}$       | <b>0.845</b>   | -0.211       | 0.030        | <b>0.885</b>          | 0.064        | 0.059        | -0.031       |
| $\text{NO}_3^-$          | 0.313  | <b>0.755</b> | 0.093        | 0.037                 | <b>0.868</b> | 0.041        | 0.271        |
| $\text{F}^-$             | 0.210  | 0.154        | <b>0.852</b> | 0.202                 | 0.164        | <b>0.827</b> | 0.300        |
| Eigen value              | 6.32   | 1.75         | 1.66         | 5.19                  | 2.68         | 1.25         | 1.19         |
| % of variance            | 48.60  | 13.48        | 12.77        | 39.89                 | 20.59        | 9.59         | 9.23         |
| Cumulative % of variance | 48.60  | 62.08        | 74.85        | 39.89                 | 60.48        | 70.07        | 79.30        |

bold values > 0.70 represent a high positive loading

**Fig. 10** (a) Principal component plot in rotated space for pre- and post-rainfall seasons. (b) Dendrogram using Ward linkage for pre- and post-rainfall seasons



**Health risk assessment (HRA)**

Hazard quotient (HQ) through ingestion ( $HQ_{ing}$ ) and dermal ( $HQ_{der}$ ) related to  $F^-$  and  $NO_3^-$  content for various age categories were estimated (U.S. EPA 2011) with the  $F^-$  and  $NO_3^-$  content values of the groundwater samples of pre- and post-rainfall seasons from the area. Parameters values used for estimating the risk of exposure to  $F^-$  and  $NO_3^-$  through ingestion and dermal pathways are presented in Table 2.

**Ingestion pathway**

In pre-rainfall season, the  $F^-$  hazard quotient values via ingestion pathway ( $HQ_{ing}$ ) for above mentioned age category i.e., 6 to 12 months, 6 to 11 years, 11 to 16 years, 16 to 18 years, 18 to 21 years, > 21 years, and > 65 years ranged from 0.51 to 10.04, 0.21 to 4.11, 0.15 to 3.06, 0.12 to 2.40, 0.16 to 3.16, 0.17 to 3.41, and 0.16 to 3.11 with mean values of 2.17, 0.88, 0.66, 0.51, 0.68, 0.73, and 0.67 (Table 7). For post-rainfall season  $F^-$  hazard quotient values via ingestion pathway

( $HQ_{ing}$ ) for different age group ranged from 0 to 0.04, 0 to 0.03, 0 to 0.025, 0 to 0.023, 0.13 to 2.53, 0.11 to 2.20, and 0.10 to 2.12 with mean values of 0.009, 0.006, 0.005, 0.0054, 0.54, 0.47, and 0.45 respectively (Table 7). The age group 6 to 12 months is observed to have highest risk due to ingestion of such  $F^-$  water, while 16 to 18 showed the least risk.

The  $NO_3^-$  hazard quotient values via ingestion pathway ( $HQ_{ing}$ ) for various age category, i.e., 6 to 12 months, 6 to 11 years, 11 to 16 years, 16 to 18 years, 18 to 21 years, > 21 years, and > 65 years ranges from 0 to 61.62, 0 to 25.26, 0 to 18.83, 0 to 14.76, 0 to 19.41, 0 to 20.92, and 0 to 19.13 with average values of 8.49, 3.48, 2.59, 2.03, 2.67, 2.88, and 2.63 for pre-rainfall season (Table 7). Similarly, for post-rainfall season, the  $NO_3^-$  hazard quotient values ( $HQ_{ing}$ ) for various age groups ranged from 0 to 41.62, 0 to 17.07, 0 to 12.72, 0 to 9.97, 0 to 13.11, 0 to 14.13, and 0 to 12.92 with average of 8.26, 3.33, 2.52, 1.97, 2.60, 2.80, and 2.56 (Table 7). The  $HQ_{ing}$  values for  $F^-$  and  $NO_3^-$  are greater than one for almost all age group of people for pre- and post-rainfall seasons. Similar to  $F^-$ ,  $NO_3^-$  also showed highest risk for age group 6 to 12 months, and least risk for 16 to 18 years.

**Table 7** Hazard quotient (HQ) for F<sup>-</sup> and NO<sub>3</sub><sup>-</sup> via ingestion (HQ<sub>ing</sub>) pathway for different age groups for pre- and post-rainfall seasons

| Age group   | Hazard quotient (HQ) via ingestion pathways for F <sup>-</sup> |       |      |   |      |      | Hazard quotient (HQ) via ingestion pathways for NO <sub>3</sub> <sup>-</sup> |      |       |   |       |      |
|-------------|--|-------|------|---|------|------|--|------|-------|---|-------|------|
|             | Pre-rainfall (HQ <sub>ing</sub> ) F <sup>-</sup>               |       |      | Post-rainfall (HQ <sub>ing</sub> ) F <sup>-</sup> |      |      | Pre-rainfall (HQ <sub>ing</sub> ) NO <sub>3</sub> <sup>-</sup>               |      |       | Post-rainfall (HQ <sub>ing</sub> ) NO <sub>3</sub> <sup>-</sup> |       |      |
|             | Min  | Ave   | SD   | Min   | Max  | SD   | Min  | Max  | SD    | Min   | Max   | SD   |
| 6–12 months | 0.51   | 10.04 | 2.17 | 1.64  | 8.10 | 1.74 | 0.37   | 8.10 | 10.40 | 0.00  | 41.62 | 9.14 |
| 6–11 years  | 0.21   | 4.11  | 0.88 | 0.67  | 3.32 | 0.71 | 0.15   | 3.32 | 4.26  | 0.00  | 17.06 | 3.74 |
| 11–16 years | 0.15   | 3.06  | 0.66 | 0.50  | 2.47 | 0.53 | 0.11   | 2.47 | 3.17  | 0.00  | 12.72 | 2.79 |
| 16–18 years | 0.12   | 2.40  | 0.52 | 0.39  | 1.94 | 0.41 | 0.08   | 1.94 | 2.49  | 0.00  | 9.97  | 2.19 |
| 18–21 years | 0.16   | 3.16  | 0.68 | 0.51  | 2.55 | 0.54 | 0.11   | 2.55 | 3.27  | 0.00  | 13.11 | 2.87 |
| > 21 years  | 0.17   | 3.41  | 0.73 | 0.55  | 2.75 | 0.59 | 0.12   | 2.75 | 3.53  | 0.00  | 14.13 | 3.10 |
| > 65 years  | 0.16   | 3.11  | 0.67 | 0.51  | 2.51 | 0.54 | 0.11   | 2.51 | 3.23  | 0.00  | 12.92 | 2.83 |

### Dermal pathway

Hazard quotient values for F<sup>-</sup> through dermal contact (HQ<sub>der</sub>) for pre-rainfall season for different age groups 6 to 12 months, 6 to 11 years, 11 to 16 years, 16 to 18 years, 18 to 21 years, > 21 years and > 65 years ranged from 0 to 0.04, 0 to 0.03, 0 to 0.02, 0 to 0.02, 0.13 to 2.53, 0.11 to 2.20, and 0.10 to 2.12 with average values of 0.009, 0.006, 0.005, 0.005, 0.54, 0.47, and 0.45, whereas for post-rainfall season (HQ<sub>der</sub>) values ranged from 0 to 0.03, 0 to 0.02, 0 to 0.02, 0 to 0.018, 0.09 to 2.04, 0.08 to 1.77, and 0.07 to 1.71 with an average value of 0.01, 0.0, 0.0, 0.0, 0.62, 0.54, and 0.52, respectively (Table 8). Similarly, for NO<sub>3</sub><sup>-</sup> in pre-rainfall season water samples through dermal contact (HQ<sub>der</sub>) for different age groups ranged from 0 to 0.26, 0 to 0.19, 0 to 0.15, 0 to 0.14, 0 to 15.55, 0 to 13.51, and 0 to 13.04 with average values of 0.03, 0.02, 0.02, 0.01, 2.14, 1.86, and 1.79 (Table 8). For post-rainfall season, the hazard quotient via dermal pathway (HQ<sub>der</sub>) for different age groups ranged from 0 to 0.17, 0 to 0.13, 0 to 0.10, 0 to 0.09, 0 to 10.50, 0 to 9.12, and 0 to 8.80 with average values of 0.03, 0.02, 0.02, 0.01, 2.08, 1.81, and 1.74 respectively (Table 8). The HQ<sub>der</sub> values for NO<sub>3</sub><sup>-</sup> are greater than for the age group of 18–21 years, > 21 years, and > 65 years for pre- and post-rainfall seasons. Hence, from this study, the HQ<sub>ing</sub> values of F<sup>-</sup> and NO<sub>3</sub><sup>-</sup> are more than that of HQ<sub>der</sub> values; hence, the ingestion pathway is more likely to cause non-carcinogenic risk to all the age group of people.

The health risk assessment results show ingestion pathway which can cause more risk than the dermal pathway. The children could be at more risk than adults due to ingestion of such high F<sup>-</sup> and NO<sub>3</sub><sup>-</sup> content water. Similarly, such results were also observed by various researchers in India (Adimalla et al. 2019; Ali et al. 2019; Adimalla 2020; Karunanidhi et al. 2020; Marghade et al. 2021; More et al. 2021; Subba Rao et al. 2019) and worldwide (Chen et al. 2017b; Gao et al. 2020; Li et al. 2019; Qasemi et al. 2018; Rehman et al. 2020; Ustaoğlu et al. 2020; Yuan et al. 2020; Zango et al. 2019).

### Remedial measures

From the present study, few valuable and simple applicable remedial measures to prevent health hazards due to the intake of high F<sup>-</sup> and NO<sub>3</sub><sup>-</sup> content water were suggested. It is suggested to supply safe drinking water to society to maintain their normal health. Provisions for denitrification and defluorination plant to reduce the F<sup>-</sup> and NO<sub>3</sub><sup>-</sup> contents in the water. Employment of rainwater harvesting structures to dilute the F<sup>-</sup> and NO<sub>3</sub><sup>-</sup> contents in the water regime. Facilitate clean and hygienic sanitary conditions in the residential areas and limitations of fertilizer use in agricultural areas.

**Table 8** Hazard quotient (HQ) for F<sup>-</sup> and NO<sub>3</sub><sup>-</sup> via dermal (HQ<sub>der</sub>) pathway for different age groups for pre- and post-rainfall seasons

| Age group   | Hazard quotient (HQ) via dermal pathways for F <sup>-</sup> |      |      |       |   |      |      |       | Hazard quotient (HQ) via dermal pathways for NO <sub>3</sub> <sup>-</sup> |       |      |      |  |       |      |      |
|-------------|---|------|------|-------|---|------|------|-------|---|-------|------|------|--|-------|------|------|
|             | Pre-rainfall (HQ <sub>der</sub> )F <sup>-</sup>             |      |      |       | Post-rainfall (HQ <sub>der</sub> ) F <sup>-</sup> |      |      |       | Pre-rainfall (HQ <sub>der</sub> )NO <sub>3</sub> <sup>-</sup>             |       |      |      | Post-rainfall (HQ <sub>der</sub> )NO <sub>3</sub> <sup>-</sup> |       |      |      |
|             | Min   | Max  | Ave  | SD    | Min   | Max  | Ave  | SD    | Min   | Max   | Ave  | SD   | Min  | Max   | Ave  | SD   |
| 6–12 months | 0.00  | 0.04 | 0.00 | 0.007 | 0.00  | 0.03 | 0.01 | 0.007 | 0.00  | 0.26  | 0.03 | 0.04 | 0.00   | 0.17  | 0.03 | 0.03 |
| 6–11 years  | 0.00  | 0.03 | 0.00 | 0.005 | 0.00  | 0.02 | 0.00 | 0.005 | 0.00  | 0.19  | 0.02 | 0.03 | 0.00   | 0.13  | 0.02 | 0.02 |
| 11–16 years | 0.00  | 0.02 | 0.00 | 0.004 | 0.00  | 0.02 | 0.00 | 0.004 | 0.00  | 0.15  | 0.02 | 0.02 | 0.00   | 0.10  | 0.02 | 0.02 |
| 16–18 years | 0.00  | 0.02 | 0.00 | 0.003 | 0.00  | 0.01 | 0.00 | 0.004 | 0.00  | 0.14  | 0.01 | 0.02 | 0.00   | 0.09  | 0.02 | 0.02 |
| 18–21 years | 0.13  | 2.53 | 0.54 | 0.41  | 0.09  | 2.04 | 0.62 | 0.44  | 0.00  | 15.55 | 2.14 | 2.62 | 0.00   | 10.50 | 2.08 | 2.30 |
| > 21 years  | 0.11  | 2.20 | 0.47 | 0.36  | 0.08  | 1.77 | 0.54 | 0.38  | 0.00  | 13.51 | 1.86 | 2.28 | 0.00   | 9.12  | 1.81 | 2.00 |
| > 65 years  | 0.10  | 2.12 | 0.45 | 0.34  | 0.08  | 1.71 | 0.52 | 0.36  | 0.00  | 13.04 | 1.79 | 2.20 | 0.00   | 8.80  | 1.74 | 1.93 |

### Conclusions

The present study is an attempt to demarcate high F<sup>-</sup> and NO<sub>3</sub><sup>-</sup> content areas and their non-carcinogenic effects on the human health of different age groups through ingestion of high contaminated water and dermal contact in the Mulugu-Venkatapur Mandals, Warangal district, Telangana India. Water samples for pre- and post-rainfall seasons were estimated for various physico-chemical parameters. Water samples are alkaline to neutral in nature. The governance of cation in water samples is in the order of Na<sup>+</sup> > Ca<sup>2+</sup> > Mg<sup>2+</sup> > K<sup>+</sup> and Ca<sup>2+</sup> > Na<sup>+</sup> > Mg<sup>2+</sup> > K<sup>+</sup> for pre- and post-rainfall seasons. Anion dominance in groundwater is of the order of Cl<sup>-</sup> > SO<sub>4</sub><sup>2-</sup> > NO<sub>3</sub><sup>-</sup>, HCO<sub>3</sub><sup>-</sup> > F<sup>-</sup> and SO<sub>4</sub><sup>2-</sup> > Cl<sup>-</sup> > HCO<sub>3</sub><sup>-</sup> > NO<sub>3</sub><sup>-</sup> > F<sup>-</sup> for pre- and post-rainfall seasons. The NO<sub>3</sub><sup>-</sup> content ranged from 0.09 to 897.28 mg/l and 0 to 606.10 mg/l, while F<sup>-</sup> content ranged from 0.28 to 5.48 mg/l and 0.21 to 4.43 mg/l for pre- and post-rainfall seasons. The WQI ranged from 18.3 to 233 and 12.97 to 219.14; 24% and 28% of samples showed excellent with WQI ≤ 50 and fit for drinking purpose, while 44% of samples showed good WQI ≥ 50 ≤ 100 and 20% and 22% shows poor water quality with WQI ≥ 200 ≤ 300 and no samples show unsuitable for drinking purposes for pre- and post-rainfall seasons. From the geochemical evolution, 46% and 51% of water samples represent carbonate type water (Ca<sup>2+</sup>.HCO<sub>3</sub><sup>-</sup>), 4% each represents non-carbonate type water (Ca<sup>2+</sup>.Cl<sup>-</sup>), and 12% of samples are non-alkali type water (Na<sup>+</sup>.Cl<sup>-</sup>), 32% and 28% groundwater samples show (Ca<sup>2+</sup>.Na<sup>+</sup>.HCO<sub>3</sub><sup>-</sup>) type water and 6% and 5% show mixed type water (Ca<sup>2+</sup>.Mg<sup>2+</sup>.Cl<sup>-</sup>) for pre- and post-rainfall seasons. The mixed water type is the dominance of (Ca<sup>2+</sup>.Mg<sup>2+</sup>.Cl<sup>-</sup>) ions which clearly specify the dominance of water–rock interaction in the aquifer system. The PCA results explained 48.60% of the total variance with strong positive loading of TDS, Ca<sup>2+</sup>, Mg<sup>2+</sup>, Na<sup>+</sup>, SO<sub>4</sub><sup>2-</sup>, and Cl<sup>-</sup> pertaining to PC1, while strong positive loading of NO<sub>3</sub><sup>-</sup> pertaining to PC2 and strong positive loading of F<sup>-</sup> pertaining to PC3. The strong positive loading of NO<sub>3</sub>

and F<sup>-</sup> pertaining to PC2 and PC3 indicates anthropogenic and geogenic contributions for increasing the concentrations in groundwater. According to the dendrogram, Cluster I, II, III, and IV was observed with a linkage distance of 5 to 25. Cluster I measured pH; cluster II measured EC, TDS, Na<sup>+</sup>, Cl<sup>-</sup> and EC, TDS, Mg<sup>2+</sup>, Na<sup>+</sup>; cluster III measured Ca<sup>2+</sup>, Mg<sup>2+</sup>, HCO<sub>3</sub><sup>-</sup> and K<sup>+</sup>, SO<sub>4</sub><sup>2-</sup>, Ca<sup>2+</sup>, Cl<sup>-</sup>, NO<sub>3</sub><sup>-</sup>; and cluster IV measured K<sup>+</sup>, SO<sub>4</sub><sup>2-</sup>, NO<sub>3</sub><sup>-</sup>, F<sup>-</sup> and HCO<sub>3</sub><sup>-</sup>, F<sup>-</sup>, CO<sub>3</sub><sup>-</sup> during pre- and post-rainfall season, respectively, indicating predominant ion exchange, silicate mineral weathering, and high uses of fertilizers.

The non-carcinogenic risk related with F<sup>-</sup> contaminated water for pre-rainfall through ingestion pathway (HQ<sub>ing</sub>) for different age groups group 6 to 12 months, 6 to 11 years, 11 to 16 years, 16 to 18 years, 18 to 21 years, ≥ 21 years, and > 65 years are ranged from 0.51 to 10.04, 0.21 to 4.11, 0.15 to 3.06, 0.12 to 2.40, 0.16 to 3.16, 0.17 to 3.41, and 0.16 to 3.11, and for post-rainfall HQ<sub>ing</sub> ranged from 0 to 0.04, 0 to 0.03, 0 to 0.025, 0 to 0.023, 0.13 to 2.53, 0.11 to 2.20, and 0.10 to 2.12. The non-carcinogenic risk associated with NO<sub>3</sub><sup>-</sup> for pre-rainfall through ingestion pathway (HQ<sub>ing</sub>) for different age groups ranged from 0 to 61.62, 0 to 25.26, 0 to 18.83, 0 to 14.76, 0 to 19.41, 0 to 20.92, and 0 to 19.13 and for post-rainfall, it ranged from 0 to 41.62, 0 to 17.07, 0 to 12.72, 0 to 9.97, 0 to 13.11, 0 to 14.13, and 0 to 12.92. HQ<sub>der</sub> values for the different age group for pre-rainfall season for F<sup>-</sup> ranged from 0 to 0.04, 0 to 0.03, 0 to 0.02, 0 to 0.02, 0.13 to 2.53, 0.11 to 2.20, and 0.10 to 2.12 and for post-rainfall season, it ranged from 0 to 0.03, 0 to 0.02, 0 to 0.02, 0 to 0.018, 0.09 to 2.04, 0.08 to 1.77, and 0.07 to 1.71. Similarly, HQ<sub>der</sub> values from NO<sub>3</sub><sup>-</sup> for different age groups for pre-rainfall season ranged from 0 to 0.26, 0 to 0.19, 0 to 0.15, 0 to 0.14, 0 to 15.55, 0 to 13.51, and 0 to 13.04 and for post-rainfall season, it ranged from 0 to 0.17, 0 to 0.13, 0 to 0/10, 0 to 0.09, 0 to 10.50, 0 to 9.12, and 0 to 8.80. HQ<sub>ing</sub> values for NO<sub>3</sub><sup>-</sup> and F<sup>-</sup> are greater than one for almost all age group of people for pre- and post-rainfall seasons; hence, there is a more probable human health risk through ingestion



pathway to all age groups of people and proper effective management measures like supply of safe drinking water, defluoridation and denitrification plants, rainwater harvesting structures, proper sanitary and waste disposal facilities, limitation use of fertilizers, and proper awareness among the localities for improving and safeguard health measures.

**Acknowledgements** The authors express their sincere gratitude to the Director, CSIR-NGRI, Hyderabad for his continuous support for the research activity. The authors express their sincere thanks to the Editor-in-Chief for his encouragement and support. The authors also thank the anonymous reviewers for their constructive and scientific suggestion for improving the manuscript standard. The manuscript reference no. is NGRI/Lib/2022/Pub-79.

**Author contribution** Ratnakar Dhakate: supervision, methodology, and original draft preparation. Shekhar More: literature collection and editing. Laxman Kumar Duvva: analyses and interpretation and literature collection. Enjamuri Satyanarayana: literature and data collection and draft preparation.

**Data availability** This is not applicable.

## Declarations

**Ethical approval** This is not applicable to this manuscript.

**Consent to participate** This is not applicable.

**Consent for publication** This is not applicable.

**Competing interests** The authors declare no competing interests.

## References

- Adimalla N, Li P (2019) Occurrence, health risks, and geochemical mechanisms of fluoride and nitrate in groundwater of the rock-dominant semi-arid region, Telangana State, India. *Hum Ecol Risk Assess an Int J* 25:81–103. <https://doi.org/10.1080/10807039.2018.1480353>
- Adimalla N, Li P, Qian H (2019) Evaluation of groundwater contamination for fluoride and nitrate in semi-arid region of Nirmal Province, South India: a special emphasis on human health risk assessment (HHRA). *Hum Ecol Risk Assess an Int J* 25:1107–1124. <https://doi.org/10.1080/10807039.2018.1460579>
- Adimalla N, Qian H (2019) Groundwater quality evaluation using water quality index (WQI) for drinking purposes and human health risk (HHR) assessment in an agricultural region of Nanganur, south India. *Ecotoxicol Environ Saf* 176:153–161. <https://doi.org/10.1016/j.ecoenv.2019.03.066>
- Adimalla N, Qian H, Nandan MJ (2020) Groundwater chemistry integrating the pollution index of groundwater and evaluation of potential human health risk: a case study from hard rock terrain of south India. *Ecotoxicol Environ Saf* 206:111217. <https://doi.org/10.1016/j.ecoenv.2020.111217>
- Adimalla N (2020) Spatial distribution, exposure, and potential health risk assessment from nitrate in drinking water from semi-arid region of South India. *Hum Ecol Risk Assess an Int J* 26:310–334. <https://doi.org/10.1080/10807039.2018.1508329>
- Ali S, Fakhri Y, Golbini M, Thakur SK, Alinejad A, Parseh I, Shekhar S, Bhattacharya P (2019) Concentration of fluoride in groundwater of India: a systematic review, meta-analysis and risk assessment. *Groundw Sustain Dev* 9:100224. <https://doi.org/10.1016/j.gsd.2019.100224>
- APHA (2012) Standard methods for the examination of water and wastewater, twenty, 2nd edn. American Public Health Association, Washington, DC
- Aydin H, Ustaoglu F, Tepe Y, Soyulu EN (2021) Assessment of water quality of streams in northeast Turkey by water quality index and multiple statistical methods. *Environ Forensics* 22:270–287. <https://doi.org/10.1080/15275922.2020.1836074>
- Bera B, Ghosh A (2019) Fluoride dynamics in hydrogeological diversity and fluoride contamination index mapping: a correlation study of North Singbhum Craton, India. *Arab J Geosci* 12:802. <https://doi.org/10.1007/s12517-019-4994-8>
- BIS (2012) Indian standards drinking water specifications IS 10500:2012. *Bur Indian Stand Indian Stand Drink Water Specif* 2:11
- CGWB (2018) Ground water quality in shallow aquifers in India. Central Ground Water Board, pp 1–218. <http://cgwb.gov.in/WQ/Ground%20Water%20Book-F.pdf>
- Chen J, Qian H, Wu H (2017a) Nitrogen contamination in groundwater in an agricultural region along the New Silk Road, northwest China: distribution and factors controlling its fate. *Environ Sci Pollut Res Int* 24:13154–13167. <https://doi.org/10.1007/s11356-017-8881-0>
- Chen J, Wu H, Qian H, Gao Y (2017b) Assessing nitrate and fluoride contaminants in drinking water and their health risk of rural residents living in a semiarid region of Northwest China. *Expo Heal* 9:183–195. <https://doi.org/10.1007/s12403-016-0231-9>
- Dhakate R, Mahesh J, Sankaran S, Gurunadha Rao VVS (2013) Multivariate statistical analysis for assessment of groundwater quality in Talcher Coalfield area, Odisha. *J Geol Soc India* 82:403–412. <https://doi.org/10.1007/s12594-013-0167-7>
- Farooq SH, Prusty P, Singh RK, et al (2018) Fluoride contamination of groundwater and its seasonal variability in parts of Purulia district, West Bengal, India. *Arab J Geosci* 11. <https://doi.org/10.1007/s12517-018-4062-9>
- Gao S, Li C, Jia C et al (2020) Health risk assessment of groundwater nitrate contamination: a case study of a typical karst hydrogeological unit in East China. *Environ Sci Pollut Res* 27:9274–9287. <https://doi.org/10.1007/s11356-019-07075-w>
- Gibbs RJ (1970) Mechanisms controlling world water chemistry. *Science* 170:795–840. <https://doi.org/10.1126/science.170.3962.1088>
- GSI (1995) Geological Survey of India's geology and minerals map of Nalgonda district. Andhra Pradesh, India
- Gugulothu S, Subba Rao N, Das R et al (2022a) Judging the sources of inferior groundwater quality and health risk problems through intake of groundwater nitrate and fluoride from a rural part of Telangana, India. *Environ Sci Pollut Res* 29:49070–49091. <https://doi.org/10.1007/s11356-022-18967-9>
- Gugulothu S, Subbarao N, Das R, Dhakate R (2022b) Geochemical evaluation of groundwater and suitability of groundwater quality for irrigation purpose in an agricultural region of South India. *Appl Water Sci* 12:142. <https://doi.org/10.1007/s13201-022-01583-w>
- Hem JD (1985) Study and interpretation of the chemical characteristics of natural water. *Reston*. <https://doi.org/10.3133/wsp2254>
- Karunanidhi D, Aravinthasamy P, Roy PD et al (2020) Evaluation of non-carcinogenic risks due to fluoride and nitrate contaminations in a groundwater of an urban part (Coimbatore region) of south India. *Environ Monit Assess* 192:102. <https://doi.org/10.1007/s10661-019-8059-y>
- Katla S, Gugulothu S, Dhakate R (2021) Spatial assessment of major ion geochemistry in the groundwater around Suryapet Region, Southern Telangana, India. *Environ Sustain* 4:107–122. <https://doi.org/10.1007/s42398-020-00148-4>
- Kechiched R, Nezli IE, Foufou A, Mohamed Salah B, Abdeldjabbar SB, Rabah D, Nacereddine S, Ouafi AZ (2020) Fluoride-bearing groundwater in the complex terminal aquifer (a case study in

- Hassi Messaoud area, southern Algeria): hydrochemical characterization and spatial distribution assessed by indicator kriging. *Sustain Water Resour Manag* 6:1–14. <https://doi.org/10.1007/s40899-020-00415-6>
- Kumar D, Singh A, Jha RK et al (2019) Source characterization and human health risk assessment of nitrate in groundwater of middle Gangetic Plain, India. *Arab J Geosci* 12:339. <https://doi.org/10.1007/s12517-019-4519-5>
- Laxmankumar D, Satyanarayana E, Dhakate R, Saxena PR (2019) Hydrogeochemical characteristics with respect to fluoride contamination in groundwater of Maheshwaram mandal, RR district, Telangana state, India. *Groundw Sustain Dev* 8:474–483. <https://doi.org/10.1016/j.gsd.2019.01.008>
- Li P, Tian R, Liu R (2019) Solute geochemistry and multivariate analysis of water quality in the Guohua Phosphorite Mine, Guizhou Province, China. *Expo Heal* 11:81–94. <https://doi.org/10.1007/s12403-018-0277-y>
- Machender G, Dhakate R, Narsimha Reddy M (2014) Hydrochemistry of groundwater (GW) and surface water (SW) for assessment of fluoride in Chinnaeru river basin, Nalgonda district, (AP) India. *Environ Earth Sci* 72:4017–4034. <https://doi.org/10.1007/s12665-014-3291-9>
- Marghade D, Malpe DB, Subba Rao N (2021) Applications of geochemical and multivariate statistical approaches for the evaluation of groundwater quality and human health risks in a semi-arid region of eastern Maharashtra, India. *Environ Geochem Health* 43:683–703. <https://doi.org/10.1007/s10653-019-00478-1>
- Mas-Pla J, Menció A (2019) Groundwater nitrate pollution and climate change: learnings from a water balance-based analysis of several aquifers in a western Mediterranean region (Catalonia). *Environ Sci Pollut Res* 26:2184–2202. <https://doi.org/10.1007/s11356-018-1859-8>
- More S, Dhakate R, Venkata Ratnal G, Machender G (2021) Hydrogeochemistry and health risk assessment of groundwater and surface water in a fluoride affected area of Yadadri-Bhuvanagiri District, Telangana State, India. *Environ Earth Sci* 80 262:1–18. <https://doi.org/10.1007/s12665-021-09544-3>
- Narsimha A, Rajitha S (2018) Spatial distribution and seasonal variation in fluoride enrichment in groundwater and its associated human health risk assessment in Telangana State, South India. *Hum Ecol Risk Assess an Int J* 24:2119–2132. <https://doi.org/10.1080/10807039.2018.1438176>
- Pérez Villarreal J, Ávila Olivera JA, Israde Alcántara I, Buenrostro Delgado O (2019) Nitrate as a parameter for differentiating groundwater flow systems in urban and agricultural areas: the case of Morelia-Capula area, Mexico. *Hydrogeol J* 27:1767–1778. <https://doi.org/10.1007/s10040-019-01933-0>
- Piper AM (1944) A graphic procedure in the geochemical interpretation of water- analyses. *Trans Am Geophys Union* 25:914–928
- Qasemi M, Afsharnia M, Farhang M et al (2018) Health risk assessment of nitrate exposure in groundwater of rural areas of Gonabad and Bajestan, Iran. *Environ Earth Sci* 77:551. <https://doi.org/10.1007/s12665-018-7732-8>
- Rehman JU, Ahmad N, Ullah N et al (2020) Health risks in different age group of nitrate in spring water used for drinking in Harnai, Balochistan, Pakistan. *Ecol Food Nutr* 59:462–471. <https://doi.org/10.1080/03670244.2020.1737044>
- Satyanarayana E, Dhakate R, Kumar DL et al (2017) Hydrochemical characteristics of groundwater quality with special reference to fluoride concentration in parts of Mulugu-Venkatapur Mandals, Warangal district, Telangana. *J Geol Soc India* 89:247–258. <https://doi.org/10.1007/s12594-017-0597-8>
- Su H, Kang W, Xu Y, Wang J (2018) Assessing groundwater quality and health risks of nitrogen pollution in the shenfu mining area of Shaanxi Province, Northwest China. *Expo Heal* 10:77–97. <https://doi.org/10.1007/s12403-017-0247-9>
- Subba Rao N, Sunithab B, Sun L et al (2019) Mechanisms controlling groundwater chemistry and assessment of potential health risk: a case study from South India. *Geochemistry* 80(4):125568. <https://doi.org/10.1016/j.chemer.2019.125568>
- Subba Rao N, Ravindra B, Wu J (2020) Geochemical and health risk evaluation of fluoride rich groundwater in Sattenapalle Region, Guntur district, Andhra Pradesh, India. *Hum Ecol Risk Assess an Int J* 26:2316–2348. <https://doi.org/10.1080/10807039.2020.1741338>
- Subba Rao N (2021) Spatial distribution of quality of groundwater and probabilistic non-carcinogenic risk from a rural dry climatic region of South India. *Environ Geochem Health* 43:971–993. <https://doi.org/10.1007/s10653-020-00621-3>
- Sudheer Kumar M, Dhakate R, Yadagiri G, Srinivasa Reddy K (2017) Principal component and multivariate statistical approach for evaluation of hydrochemical characterization of fluoride-rich groundwater of Shaslar Vagu watershed, Nalgonda District, India. *Arab J Geosci* 10:83. <https://doi.org/10.1007/s12517-017-2863-x>
- Tasa B, Tepe Y, Ustaoglu F, Alptekin S (2019) Benthic algal diversity and water quality evaluation by biological approach of turnasuyu creek, ne turkey. *Desalin Water Treat* 155:402–415. <https://doi.org/10.5004/dwt.2019.24225>
- Ustaoglu F, Tepe Y (2019) Water quality and sediment contamination assessment of Pazarsuyu Stream, Turkey using multivariate statistical methods and pollution indicators. *Int Soil Water Conserv Res* 7:47–56. <https://doi.org/10.1016/j.iswcr.2018.09.001>
- Ustaoglu F, Tepe Y, Taş B (2020) Assessment of stream quality and health risk in a subtropical Turkey river system: a combined approach using statistical analysis and water quality index. *Ecol Indic* 113:105815. <https://doi.org/10.1016/j.ecolind.2019.105815>
- U.S. EPA (2011) Exposure factors handbook 2011 edition (Final Report). U.S. Environmental Protection Agency, Washington, DC, EPA/600/R-09/052F. <https://cfpub.epa.gov/ncea/risk/recordisplay.cfm?deid=236252>
- Wu J, Li P, Wang D et al (2020) Statistical and multivariate statistical techniques to trace the sources and affecting factors of groundwater pollution in a rapidly growing city on the Chinese Loess Plateau. *Hum Ecol Risk Assess an Int J* 26:1603–1621. <https://doi.org/10.1080/10807039.2019.1594156>
- Yousefi M, Ghoochani M, Hossein Mahvi A (2018) Health risk assessment to fluoride in drinking water of rural residents living in the Poldasht city, Northwest of Iran. *Ecotoxicol Environ Saf* 148:426–430. <https://doi.org/10.1016/j.ecoenv.2017.10.057>
- Yuan L, Fei W, Jia F et al (2020) Health risk in children to fluoride exposure in a typical endemic fluorosis area on Loess Plateau, north China, in the last decade. *Chemosphere* 243:125451. <https://doi.org/10.1016/j.chemosphere.2019.125451>
- Zango MS, Sunkari ED, Abu M, Lermi A (2019) Hydrogeochemical controls and human health risk assessment of groundwater fluoride and boron in the semi-arid North East region of Ghana. *J Geochemical Explor* 207:106363. <https://doi.org/10.1016/j.gexplo.2019.106363>
- Zhang M, Huang G, Liu C et al (2020) Distributions and origins of nitrate, nitrite, and ammonium in various aquifers in an urbanized coastal area, south China. *J Hydrol* 582:124528. <https://doi.org/10.1016/j.jhydrol.2019.124528>

**Publisher's note** Springer Nature remains neutral with regard to jurisdictional claims in published maps and institutional affiliations.

Springer Nature or its licensor (e.g. a society or other partner) holds exclusive rights to this article under a publishing agreement with the author(s) or other rightsholder(s); author self-archiving of the accepted manuscript version of this article is solely governed by the terms of such publishing agreement and applicable law.

## Authors and Affiliations

Ratnakar Dhakate<sup>1,2</sup> · Shekhar More<sup>1,2</sup> · Laxman Kumar Duvva<sup>3</sup> · Satyanarayana Enjamuri<sup>4</sup>

Shekhar More  
shekharmore4444@gmail.com

Laxman Kumar Duvva  
laxman.d09@gmail.com

Satyanarayana Enjamuri  
sathishv36@gmail.com

<sup>2</sup> Academy of Scientific and Innovative Research (AcSIR),  
Ghaziabad 201002, India

<sup>3</sup> Centre for Environment, Jawaharlal Nehru Technological  
University, Hyderabad 500 085, Telangana, India

<sup>4</sup> Groundwater Department, Telangana State,  
500004 Hyderabad, Telangana, India

<sup>1</sup> CSIR-National Geophysical Research Institute, Uppal Road,  
Hyderabad 500007, Telangana, India